CAPITAL UNIVERSITY OF SCIENCE AND TECHNOLOGY, ISLAMABAD

Design, Development, and Characterization of Stimuli-Responsive Polymeric Carriers for Colon-Specific Drug Delivery: A Promising Approach for Capecitabine

by

Sohail Akram

A thesis submitted in partial fulfillment for the degree of Master of Philosophy

in the

Faculty of Pharmacy
Department of Pharmaceutics

2025

This thesis is dedicated to my parents, family, friends, and my teachers who supported me throughout every phase of my life. Without their support, this journey would not have been possible.

CERTIFICATE OF APPROVAL

Design, Development, and Characterization of Stimuli-Responsive Polymeric Carriers for Colon-Specific Drug Delivery: A Promising Approach for Capecitabine

by

Sohail Akram

(Registration No: MPH233006)

THESIS EXAMINING COMMITTEE

S. No.	Examiner	Name	Organization
(a)	External Examiner	Dr. Shahiq Uz Zaman	RIU, Islamabad
(b)	Internal Examiner	Dr. Mahira Zeeshan	CUST, Islamabad
(c)	Supervisor	Dr. Nadia Shamshad Malik	CUST, Islamabad

Dr. Nadia Shamshad Malik
Thesis Supervisor
October, 2025

Dr. Nadia Shamshad Malik
Head
Dept. of Pharmaceutics
October, 2025

Dr. Muzaffar Abbas
Dean
Faculty of Pharmacy
October, 2025

Author's Declaration

I, **Sohail Akram** hereby state that my MS thesis titled "**Design, Development, and Characterization of Stimuli-Responsive Polymeric Carriers for Colon-Specific Drug Delivery: A Promising Approach for Capecitabine**" is my own work and has not been submitted previously by me for taking any degree from Capital University of Science and Technology, Islamabad or anywhere else in the country/abroad.

At any time if my statement is found to be incorrect even after my graduation, the University has the right to withdraw my MPhil Degree.

(Sohail Akram)

Registration No: MPH233006

Plagiarism Undertaking

I solemnly declare that research work presented in this thesis titled "**Design, Development, and Characterization of Stimuli-Responsive Polymeric Carriers for Colon-Specific Drug Delivery: A Promising Approach for Capecitabine**" is solely my research work with no significant contribution from any other person. Small contribution/help wherever taken has been duly acknowledged and that complete thesis has been written by me.

I understand the zero tolerance policy of the HEC and Capital University of Science and Technology towards plagiarism. Therefore, I as an author of the above titled thesis declare that no portion of my thesis has been plagiarized and any material used as reference is properly referred/cited.

I undertake that if I am found guilty of any formal plagiarism in the above titled thesis even after award of MPhil Degree, the University reserves the right to withdraw/revoke my MPhil degree and that HEC and the University have the right to publish my name on the HEC/University website on which names of students are placed who submitted plagiarized work.

(Sohail Akram)

Registration No: MPH233006

List of Publications

It is certified that following publication(s) have been made out of the research work that has been carried out for this thesis:-

1. **Akram, S.**, Malik, N. S., Zeeshan, M., Tulain, U. R., Anwar, M., Mahmood, A., ... & Rahman, A. U. (2025) "Design, development, and characterization of stimuli-responsive polymeric carriers for colon-specific drug delivery: A promising approach for capecitabine," *Journal of Drug Delivery Science and Technology*, vol. 113, 107359.

(Sohail Akram)
Registration No: MPH233006

Acknowledgement

First and foremost, I am profoundly grateful to Allah, the Most Gracious and the Most Merciful, for granting me the strength, perseverance, and wisdom to complete this academic endeavor. His divine guidance has been a constant source of support throughout this journey.

I would like to express my sincere appreciation to Dr. Nadia Shamshad Malik, my research supervisor, for her invaluable guidance, continuous encouragement, and constructive feedback throughout the course of this study. Her expertise, insightful suggestions, and unwavering support were critical to the successful completion of this thesis. Her dedication to academic excellence and mentorship influenced the quality and direction of my research.

I extend my heartfelt thanks to my family, whose unwavering support, encouragement, and belief in my potential have been a constant source of motivation. Their patience and understanding provided me with the emotional strength needed to navigate this journey.

My sincere gratitude also goes to my research group colleagues and peers, whose collaboration, thoughtful discussions, and shared commitment to academic growth created a stimulating and supportive research environment.

I am also thankful to my friends, whose encouragement, positivity, and timely support brought balance and joy throughout this academic pursuit.

Lastly, I gratefully acknowledge my institute for providing the academic platform, resources, and conducive research environment that made this work possible. The infrastructure and administrative support played a significant role in facilitating various aspects of my research.

(Sohail Akram)

Abstract

Colorectal cancer remains one of the leading causes of cancer-related mortality worldwide, underscoring the urgent need for advanced drug delivery systems that enhance therapeutic efficacy while minimizing systemic toxicity. In this study, pH-responsive hydrogel-based polymeric carriers were developed and characterized for the delivery of capecitabine (CT), a chemotherapeutic drug used to treat colorectal cancer. Hydrogels were synthesized by crosslinking synthetic (cellulose acetate phthalate) and natural (pectin, guar gum) polymers to confer pH-sensitive behavior. A total of eleven formulations (F1–F11) were evaluated for encapsulation efficiency (EE%), swelling behavior, and in vitro drug release under simulated gastrointestinal conditions (pH 1.2 and 7.4). Among these, the optimized formulation F5 demonstrated superior performance, achieving EE% values of 62.00 ± 0.85% at pH 1.2 and 86.49 ± 0.94% at pH 7.4, indicating effective gastric protection and enhanced colonic targeting. Swelling studies confirmed pH-dependent expansion, with a swelling index of 76.70% at pH 7.4 and negligible swelling at pH 1.2. In vitro release studies showed sustained CT release over 24 hours, with 62% release at pH 1.2 and 86% at pH 7.4. The release kinetics followed the Korsmeyer–Peppas model ($R^2 = 0.996$, $n = 0.565$), suggestive of anomalous (non-Fickian) transport. Physicochemical characterizations confirmed successful drug encapsulation and polymer compatibility via FTIR, while SEM analysis revealed a porous hydrogel architecture. Furthermore, DSC and XRD analyses indicated the amorphous dispersion of CT within the polymeric matrix. Acute oral toxicity studies conducted in mice demonstrated the hydrogel's biocompatibility, with no significant alterations in hematological, biochemical, or histopathological parameters. These findings establish formulation F5 as a promising colon-targeted drug delivery system for capecitabine, capable of enhancing therapeutic outcomes, reducing dosing frequency, and minimizing systemic toxicity. This study supports the potential of pH-responsive hydrogels as effective platforms for colorectal cancer therapy.

Keywords Hydrogel, Capecitabine, Pectin, Guar Gum, Colon-Targeted Delivery, Cellulose Acetate Phthalate

Contents

List of Figures

List of Tables

Abbreviations

AA	Acrylic Acid
ALP	Alkaline Phosphatase
ALT	Alanine Aminotransferase
ANOVA	Analysis of Variance
APS	Ammonium Per sulfate
AST	Aspartate Aminotransferase
BCS	Biopharmaceutics Classification System
CAP	Cellulose Acetate Phthalate
CRC	Colorectal Cancer
CT	Capecitabine
DL	Drug Loaded
DLS	Dynamic Light Scattering
DSC	Differential Scanning Calorimetry
EDTA	Ethylenediaminetetraacetic Acid
EE	Encapsulation Efficiency
FTIR	Fourier Transform Infrared Spectroscopy
FDA	Food and Drug Administration
GG	Guar Gum
GRAS	Generally Recognized as Safe
K_2HPO_4	Dipotassium Hydrogen Phosphate
KH_2PO_4	Potassium Dihydrogen Phosphate
LC	Loading Capacity
m^2	Square Meter

M	Molar
MBA	N,N-Methylenebisacrylamide
mg	Milligram
mL	Milliliter
mV	Millivolt
N	Normal
NaOH	Sodium Hydroxide
PEC	Pectin
R^2	Regression Coefficient
SD	Standard Deviation
SEM	Scanning Electron Microscopy
UV	Ultraviolet
XRD	X-ray Diffraction

Chapter 1

Introduction

1.1 Overview of Colorectal Cancer and Therapeutic Challenges

1.1.1 Epidemiology and Burden of Colorectal Cancer

Colorectal cancer (CRC) is a critical health problem worldwide, being one of the most widespread and fatal cancers. It impacts people of all ages and begins in the colon or rectum. It is the third most commonly diagnosed cancer, and it comes second in the list of the most cancerous deaths with about 1.9 million new cases and 935,000 deaths in the year 2020 (WHO, 2021). This disease is more prevalent in developed countries, such as the US, Canada, Australia, and European nations [1]. Colorectal cancer is increasingly becoming a prominent public health challenge in Pakistan, with rising incidence rates in the past decades. Recent epidemiological studies show that colorectal cancer constitutes 4-5% of the total cancer burden in Pakistan, which places Pakistan among the top five countries in the world with the highest prevalence rate of this disease among men and women. Pakistan's estimated age-standardised incidence rate (ASIR) for colorectal cancer is approximately 7.5 per 100,000 population [2]. This is commonly associated with lifestyle risk factors including: smoking, excessive red or processed meat

consumption, lack of fibre consumption, obesity, no physical activity, alcohol, and smoking. However, even in developing countries, there is now a surge in cases. This has been associated with an increase in non-communicable diseases, such as cancer. Nonetheless, there is considerable promise in the form of pH-sensitive hydrogels, which provide novel and innovative approaches to resolving this global concern [3].

CRC primarily affects individuals aged 50 and above, but recent cases have also been detected in people younger than 50. It is particularly troubling as younger patients tend to have more advanced-stage disease during diagnosis. It poses immense strain on the healthcare systems owing to the expensive treatments, hospital stays, and prolonged recovery periods. Apart from the pain, there is so much emotional distress to the patients and families involved. Screening programs, like colonoscopy and stool-based tests, are designed to help detect CRC at an early stage, which improves the chances of better outcomes. Unfortunately, these services are not readily available in rural or low socio-economic areas, resulting in delayed detection and poorer outcomes [4].

The alarming burden of CRC placed on the healthcare structures underscores the urgent need for a reduction in drug delivery systems. An ideal delivery system would avoid other organs, enabling direct transport to the colon while allowing for controlled release of medication to minimise some side effects and improve the efficacy of treatment. The creation of such systems should be a higher-priority area of study [5].

Colorectal cancer (CRC) involves the transformation and abnormal proliferation of rectal and large bowel tissue cells and is considered one of the most widely diagnosed malignancies among men and women. Cancer cells can potentially spread to distant areas of the body, causing new metastatic cancer [6].

Adenocarcinoma, squamous cell carcinoma, extranodal NK/T cell lymphoma, not otherwise specified, large B cell lymphoma, and MALT lymphoma are the major subtypes of CRC. In adults younger than 50, CRC develops more often and is occasionally identified when the patient is still in their 20s. A medical consultation

is the first step in diagnosing the disease, which includes a physical exam and checking a family's medical history. Most treatments use a combination of surgery, radiation therapy, and chemotherapy to eliminate the tumor [7].

Carcinoma, due to tumors that occur in the cells covering the length of the rectum and colon, is known as colorectal cancer. The term "colon" encompasses several parts, including the ascending colon or right colon, which is where the appendix is located, the transverse colon, the descending or left colon, and ultimately the sigmoid colon, which contains a large amount of stool. The final portion of the large bowel before stool is released into the anus is the rectum [8]. By causing necrosis and tissue breakdown in the colon wall, CRC can elicit cancer obstruction.

The number of infections, mortalities, and disabilities from CRC is predicted to rise because of these factors. Community awareness and knowledge about the causes and effective treatments for diseases, as well as any available preventive measures, can make a significant difference. Many factors can increase the risk of CRC occurring, but the risk can be mitigated by a strategy of early detection, diagnosis, and selection of a therapy that matches the patient's needs [9].

1.1.2 Clinical Challenges in Current CRC Therapies

Colorectal cancer is typically treated with a combination of surgery, chemotherapy, radiation, and targeted therapy. If the cancer is diagnosed early, surgery alone canbe sufficient to clear the tumor. But in most cases, the disease is found at an advanced stage, and the patients need further treatments, such as chemotherapy or radiation. Chemotherapy uses strong medications to kill or slow the growthof cancer cells. 5-fluorouracil (5-FU), oxaliplatin, and irinotecan are the generaldrugs for CRC [10]. These drugs are generally injected, but some can be ingested. Chemotherapy can be successful, but it is highly toxic because it damages healthy cells, too. Patients frequently feel nauseous, lose their hair, become tired, and have a compromised immune system. These side effects can be difficult to control, particularly for elderly patients and those with other health conditions [11].

Chemotherapy drugs do not always reach the tumor in high enough amounts. A significant portion of the drug is absorbed or destroyed before it reaches the colon. This means the patient must take a larger dose, which raises the level of drugs in the body and increases the chances of side effects. This is especially pertinent with drugs that are already known to produce dangerous or toxic side effects. Tumors can also, and often do, become resistant to chemotherapy, or the cancer may return after a short period (rebound cancer) [12]. Radiation therapy is another option for mainly rectal cancer. Radiation therapy works by using high-energy rays to kill cancer cells. While radiation can and does work by damaging the DNA of cancer cells enough that they cannot repair themselves, it also damages healthy DNA and tissues. Radiation therapy affects nearby healthy tissues, which is often a significant downside to the treatment. Targeted therapy and immunotherapy are currently being explored as potential enhancements to existing treatments. These treatments are meant to "train" the body's immune system to work harder against the cancer cells or to directly target only the cancer cells while sparing nearby healthy tissue. Less immune-suppressing, less risky, and less weighty treatment would be a huge step forward [13].

1.2 Chemotherapy and Targeted Therapies

Nowadays, in addition to surgery, which continues to be an irreplaceable treatment for colorectal carcinoma, the role and importance of systemic chemotherapy are gradually increasing [14]. The commonly used chemotherapy agents include fluorouracil, capecitabine, raltitrexed, tegafur, irinotecan, and oxaliplatin, among which biochemical application-based fluorouracil is the most widely used. With the continuous deepening of the study on the pathogenesis of colorectal cancer, many new chemotherapeutic agents that can specifically target biological markers such as vascular endothelial growth factor and epidermal growth factor receptor in the pathogenesis process of colorectal carcinoma have successively entered the stage of clinical use and have shown the ability to change the pattern of the colorectal cancer treatment concept [15].

The role of chemotherapy in the treatment of colorectal carcinoma may be reflected in the following aspects: neoadjuvant chemotherapy can reduce the size of preoperative local tumors and the lymph node infiltration rate of surgical specimens, thus improving the surgical curability rate; perioperative systemic chemotherapy is helpful to eliminate surgical micro metastasis and inhibit angiogenesis; adjuvant chemotherapy regimens implemented after surgery can eliminate postoperative micro metastases, reduce the possibility of recurrence and metastasis, and improve disease-free and overall survival rates; for advanced colorectal carcinomas that are not suitable for surgical resection, systemic chemotherapy and targeted drug protocols for tumors are highlights in these cancers' chemo-based interventions [16]. The commonly used chemotherapy drugs for colorectal carcinoma and their main action mechanisms are as follows: chemotherapy drugs for treating colorectal cancer. Combination chemotherapy is commonly used clinically to achieve the effect of comprehensive killing of tumor cells and reducing drug resistance [17].

1.3 Stimuli-Responsive Drug Delivery: pH as a Key Trigger for Colon Targeting

Scientists are developing new methods to deliver drugs with greater accuracy. One such method, known as a stimulus-responsive drug delivery system, releases medication only when it detects specific conditions within the body, such as pH changes, temperature fluctuations, enzyme presence, or pressure shifts. The conditions mentioned above serve as "triggers" to activate the release of the drug. In the context of colon-targeted drug delivery, pH is not just a valid trigger; it's a game-changer [18]. The varying pH levels of the digestive tract can be used to construct systems that remain solid in both the stomach and small intestine yet dissolve in the colon, representing a significant leap forward in drug delivery innovation. In these systems, we use materials that dissolve at high pH levels. One example is Eudragit S100, a commonly used polymer that remains stable in acidic conditions but dissolves at a pH above 7. This means that the drug inside

remains protected during its journey through the upper digestive system and is only released when it reaches the colon. Using pH as a trigger for drug release in systems targeting the colon offers many advantages [19].

However, it is a straightforward system to set up because only one polymer is needed to mix with the drug at a specific point in time. This can be achieved in various forms, such as tablets, capsules, or hydrogels. Indeed, these are inexpensive and simple to manufacture, and they can easily be modified to fit various drugs. Furthermore, they prevent the medications from releasing too early, while ensuring the drugs have sufficient potency to reach the colorectal cancer site before being used up [20].

1.4 Hydrogels as Smart Carriers for Colon-Targeted Chemotherapy

Hydrogels are soft, flexible materials that can absorb a significant amount of water. They are made from polymers that form a three-dimensional structure. Hydrogel products already include contact lenses and wound dressings. Over the past few years, the use of these versatile materials in medicine has increased significantly, particularly for drug delivery applications [21]. One type of hydrogel used in medical applications is sensitive to pH, swelling, and shrinking in response to the pH of its environment. For applications in the colon, the pH-sensitive hydrogel is designed to remain compact in the stomach and small intestine but to swell and release its payload in the colon [22]. Hydrogels can carry both water-loving (hydrophilic) and water-hating (hydrophobic) drugs. They can be formed from natural materials, like chitosan, or from synthetic ones, like polyacrylic acid. In treating cancer, hydrogels can serve as a delivery mechanism that releases a drug slowly over time, keeping its concentration in the body at a stable level. This, of course, is advantageous compared to administering the medicine in a series of bolus doses [23]. The benefits of hydrogels include the absorption of the drug at the intended site in the colon, enhanced retention time in the colon, and the possible

use of biodegradable hydrogels in colorectal cancer therapy. Site-specific, sustained release of the drug from hydrogels can be achieved when they are designed to respond to local conditions (e.g., pH). Additionally, the use of chemotherapy drugs carried by hydrogels is also possible in the same therapy [24].

1.5 Rationale and Objectives of the Present Study

1.5.1 Rationale for Developing pH-Sensitive Hydrogels

Colorectal cancer (CRC) remains a major global health concern, characterized by high mortality rates and limited treatment efficacy, particularly in advanced stages. Conventional drug delivery systems often fail to achieve targeted localization of chemotherapeutic agents within the colon due to premature drug release, degradation in the gastric environment, or systemic absorption in the upper gastrointestinal tract. These limitations result in subtherapeutic drug concentrations at the tumor site and increased systemic toxicity. To address these challenges, pH-sensitive hydrogels have emerged as a promising drug delivery platform [25]. These systems remain stable in the acidic environment of the stomach and the mildly acidic pH of the small intestine but undergo swelling and drug release in the alkaline pH of the colon. This mechanism ensures site-specific delivery, thereby enhancing therapeutic efficacy while minimizing off-target effects [26]. The development of hybrid hydrogels composed of both natural (e.g., pectin, guar gum) and synthetic (e.g., cellulose acetate phthalate, methacrylic acid) polymers further improve the biocompatibility, mechanical strength, and controlled-release properties of the system. Such polymeric networks offer enhanced stability, pH-responsiveness, and tunable degradation profiles, making them suitable for colon-targeted delivery of anticancer agents like Capecitabine. Given the limitations of current treatment approaches and the growing interest in localized drug delivery technologies, this study is designed to develop and evaluate a pH-sensitive hydrogel formulation for

site-specific and sustained release of Capecitabine. This strategy is expected to optimize therapeutic outcomes and reduce systemic toxicity, thereby improving the overall safety and efficacy of CRC management [27].

To our knowledge, this is the first study of a CAP-pectin-guar gum ternary hydrogel system that harnesses the complementary advantages of natural and synthetic polymers, while eliminating the need for toxic crosslinking agents and simplifying the fabrication process.

The designed hydrogel system is intended to minimize premature drug release in the upper gastrointestinal tract, enable controlled and sustained capecitabine release within the colon, and ultimately reduce dosing frequency and systemic side effects.

This colon-targeted delivery platform holds promises for enhancing patient compliance, therapeutic efficacy, and overall quality of life in CRC patients.

1.5.2 Research Objectives and Hypothesis

This research has the following main objectives:

1. Design and formulate a hydrogel system incorporating Capecitabine using a combination of pectin, guar gum, cellulose acetate phthalate, and acrylic acid.

2. Address the challenges of Capecitabine, such as limited solubility, short half-life by enhancing drug delivery through the hydrogel.

3. Investigate the role of each polymer in the formulation to ensure effective pH-responsive behavior and controlled drug release.

4. Characterize the physicochemical properties of hydrogel, including swelling behavior, mechanical strength, and drug release profile.

5. Conduct in vitro studies to analyze the release kinetics of Capecitabine under various pH conditions.

6. Evaluate the biosafety of the formulated hydrogel system by conducting oral acute toxicity study via OECD guidelines.

The proposed pH-sensitive hybrid hydrogel, composed of both natural and synthetic polymers, is expected to facilitate site-specific and sustained delivery of Capecitabine to the colon. This targeted delivery system is anticipated to enhance drug bioavailability, overcome limitations related to solubility and short half-life, and reduce systemic toxicity. Furthermore, the hydrogel is expected to demonstrate a favorable safety profile, as confirmed through in vitro release kinetics and oral acute toxicity studies conducted in accordance with OECD guidelines.

Chapter 2

Literature Review

2.1 Advances and Limitations in Oral Chemotherapy for Colorectal Cancer

In the last couple of decades, treating colorectal cancer (CRC) has heavily relied on chemotherapy techniques. Most drugs are administered via injections at hospitals, which can be both uncomfortable and time-consuming for patients. To address these challenges, researchers have developed oral chemotherapy medications.

These can be taken orally, which means patients do not have to visit hospitals for treatments. An example of such medicines is capecitabine, which is widely used for treating colorectal cancer (CRC). Its mode of action involves transforming into an active compound that fights cancerous cells within the body and directly attacks the tumor cells [28]. As advantageous as these medications may seem, oral chemotherapy poses numerous complications.

Several factors detract from their overall efficacy. One of its most prominent issues is low bioavailability, meaning only a small portion of the medicine enters circulation and reaches the cancerous tissues. Many medications disintegrate in the stomach due to harsh acids or digestive enzymes, thus posing barriers that can prevent the entire drug dose from traversing the upper digestive tract unscathed.

Even if the drug is absorbed, it might reach the colon before it is typically absorbed in the small intestine, which is the typical site for most cancers.

Another dilemma relates to first-pass metabolism, which happens when a drug is broken down by the liver before it has a chance to enter the systemic circulation. The liver has the capability of modifying or synthesizing the medication, and in doing so, reduces its efficacy. This means that, often, the doses must be increased, which has a negative impact, including side effects such as fatigue, vomiting, diarrhea, and suppression of the immune system. These side effects can diminish a patient's life experience and at times, lead to therapy stopping midway.

To rectify the problems mentioned above, scientists have considered strategies to shield oral formulations from early breakdown. Some of them utilize medically approved coatings, such as enteric coatings or capsules, that dissolve at higher pH levels. These instruments aim to shield the therapeutics from gastric acids and deliver them to the distal parts of the gut.

Still, even these systems do not always work because the levels of acid in the stomach and the rate of food transit in the intestines are different from individual to individual. Hence, there is no guarantee that every patient can be that the drug will reach the colon. Therefore, it is clear that a better solution is needed that ensures the drug remains safe as it travels through the digestive system and then releases it specifically in the colon [29].

2.2 Colon-Targeted Strategies: pH Sensitive Systems in Focus

To improve the treatment for colorectal cancer, researchers have created methods for colon-specific drug delivery that administer medication straight to the colon. This method, colon-targeted drug delivery, is essential because the medication can be given precisely where the tumor is located. This technique reduces injury to healthy tissues and enables lower dosage, which is less likely to produce adverse

effects [30]. There are three primary types of colon-targeted drug systems: time-release, enzyme-activated, and pH-sensitive systems. The first type, time-based systems, releases the drug after a predetermined time has passed. The notion is that if the drug is held intact for several hours, it will eventually reach the colon.

However, this approach has not been too successful. The rate at which food or medication moves through the digestive tract differs from one individual to another. For instance, a person who consumes a large meal is likely to take much longer to empty their bowel than someone hungry. When combined, the medication may be released either too early or too late as a consequence [31].

The second approach relies on the action of colon bacteria and their enzymes. Some components, like starch, pectin, or guar gum, which are not utilized by the bacteria until they reach the colon, are included in these enzyme-responsive systems. The drug is released when the material is degraded. This approach works well when the patient has a robust gut flora.

However, in cancer patients or those who have taken some antibiotics, the bacterial count may be suboptimal, which affects the reliability of the system [32]. The third and most advanced is the one that utilizes a pH-sensitive system. This method takes advantage of the fact that pH, which measures how acidic or basic something is, varies in different parts of the digestive system [33].

The stomach is very acidic at about 1–3 pH. The small intestine is less acidic, with a range of pH 5 to 6.5, while the colon is weakly alkaline with a pH of 6.8 to 7.8. Scientists can use materials that only dissolve at a specific pH in order to design the drug formulation for protection in the stomach and small intestine and dissolution and release in the colon [34].

Materials like Eudragit S100, hydroxypropyl methylcellulose phthalate, and cellulose acetate phthalate are used for this purpose. These polymers remain solid in acidic environments but dissolve when the pH reaches approximately 7.0 [35]. Laboratory studies and clinical trials have demonstrated that pH-sensitive systems are more consistent and easier to control than time-based or enzyme-based

systems [36]. Hence, they are a preferred choice for colon cancer drug delivery today [37].

2.3 pH-Responsive Hydrogels: Swelling Behavior and Drug Release Kinetics

One exemplary class of pH-sensitive systems is Hydrogel. Hydrogels are soft, sponge-like structures prepared from polymers that have the capability of absorbing large quantities of water or any other fluid. The greater segment of hydrogels is utilized in dense drug delivery systems. For these hydrogels, the size and shape, as well as the dimension of such systems, transform based on the pH level of the pH regulators in question. This remarkable feature is essential in controlling the specific site and timing of drug release. In the case of acidic surroundings, such as the stomach, pH-sensitive hydrogels remain in a compressed and tight form to prevent drugs from leaking out [38]. When hydrogels advance towards the small intestine and later into the colon, where the basic PH becomes higher, the material commences swelling, thereby enabling the drug to be released separately in that region. Such mechanisms are described as swelling-based drug release methods [39].

The swelling of a hydrogel and the rate of drug release are dependent on multiple factors, such as the polymer type, cross-linking degree, and gel thickness. High cross-linking yields more rigid hydrogels that swell less and release drugs at slower rates, while lower cross-linking leads to softer hydrogels that swell and release drugs quickly. The release kinetics of the drug from hydrogels are studied using simple mathematical models [40]. The slow movement of molecules within the puffed gel structure is described by the Higuchi model concerning drug release [41]. This model also incorporates drifting due to both swelling and erosion, using the Korsmeyer-Peppas model, thus providing an understanding of the controlling mechanisms behind the release. Through these models, researchers can construct appropriate hydrogels that release the drug at the right time and level

[42]. Achieving efficiency for colon cancer with hydrogel requires three attributes. To begin with, the hydrogel must maintain its stability in the stomach in order to prevent the premature loss of the medicine. It must also swell partially in the small intestine. Lastly, it must swell completely in the colon for the drug release. Monitoring these factors can greatly reduce the side effects while using lower doses of the drug, which improves the overall results of the treatment [43].

2.4 Natural and Synthetic Polymers in Hydrogel Design

A useful approach to hydrogels with more pH-responsive properties for colon-targeted drug delivery systems could be the blend of natural and synthetic polymers. Among synthetic polymers, cellulose acetate phthalate (CAP) has a prominent position because it is widely used in pharmaceutical formulations as an enteric coating material. CAP is stable and insoluble in acidic conditions like the stomach, which avoids the premature release of the drug. It, however, is suitable for higher pH regions like those in the small intestine and colon, which is where site-specific drug release can happen. This property of CAP is advantageous for formulations meant to bypass the upper gastrointestinal (GI) tract and be released selectively in the lower GI tract, including the colon [44]. To further enhance the biocompatibility and functionality of the hydrogel, natural polymers such as pectin and guar gum are incorporated into the matrix. These biopolymers not only improve the environmental safety and degradability of the hydrogel but also contribute unique physicochemical characteristics that support colon-targeted drug delivery. Pectin, an anionic polysaccharide derived primarily from plant cell walls, contains ionizable groups (e.g., carboxyl groups) that exhibit pH-sensitive swelling behavior [45]. In the neutral to slightly alkaline environment of the colon, these groups become ionized, leading to hydrogel swelling and facilitating the controlled release of the encapsulated drug. Moreover, pectin participates in the hydrogel network formation through electrostatic interactions and hydrogen bonding, thereby reinforcing

the structural integrity of the matrix [46]. Guar gum, a galactomannan polysaccharide extracted from guar beans, further enhances the mechanical strength and cohesiveness of the hydrogel. Though it is a nonionic polymer, it contributes to matrix stability and viscosity. Its mucoadhesive properties are especially advantageous for prolonged retention at the target site within the colon, enabling sustained and localized drug delivery. This attribute is essential for increasing the bioavailability of poorly absorbed drugs and reducing systemic side effects [46]. The inclusion of acrylic acid (AA), a pH-sensitive monomer, significantly augments the responsiveness of the hydrogel to pH changes along the GI tract. MAA contains carboxylic acid groups that remain protonated and uncharged in acidic environments, thereby limiting water uptake and swelling in the stomach. However, upon reaching higher pH conditions, such as those in the colon, these carboxyl groups ionize to form carboxylate anions. This ionization induces substantial swelling of the hydrogel matrix, promoting the controlled and site-specific release of the encapsulated drug. MAA thus provides an additional layer of pH-triggered control, complementing the properties of CAP and the natural polymers [25]. The rationale behind this multi-polymeric system is to design a hydrogel with robust pH-sensitivity, mucoadhesiveness, and biodegradability, tailored for colon-specific drug delivery. By combining the enteric properties of CAP, the biocompatibility and swelling behaviors of pectin and guar gum, and the sharp pH-responsiveness of MAA, the hydrogel can effectively protect the drug from premature release in the stomach and small intestine. At the same time, it ensures a sustained and targeted release upon reaching the colon. This innovative hydrogel system holds significant therapeutic potential. It addresses several critical challenges in oral drug delivery, including drug degradation in the stomach, poor drug absorption, and frequent dosing. By minimizing premature release and enabling prolonged, localized delivery in the colon, such systems can enhance therapeutic efficacy, reduce dosing frequency, and ultimately improve patient adherence and outcomes in the treatment of chronic colonic diseases such as ulcerative colitis, Crohn's disease, and colorectal cancer [25]. Table 2.1 depicts polymers that were used for hydrogel preparation.

TABLE 2.1: Polymers Used for Hydrogel Preparation

Polymers Used	Properties	Mechanism of pH-Responsiveness	Findings/Applications	Reference
Cellulose Acetate Phthalate (CAP)	Synthetic polymer, Enteric coating properties, Acid-resistant, and dissolves at higher pH	Remains intact in stomach (pH 1-3). Dissolves in intestinal/colonic pH (≥6.8)	Ideal for preventing gastric drug release	[44]
			Ensures targeted colonic delivery	
Pectin (anionic polysaccharide)	Biocompatible	Electrostatic interactions in hydrogel	Enhances controlled drug release in the colon	[45]
	pH-sensitive Swellable in colonic pH	Ionizable groups (COOH) deprotonate at higher pH, increasing swelling	Improves crosslinking	
Guar Gum (neutral polysaccharide)	Mucoadhesive	Forms a cohesive hydrogel matrix	Improves sustained drug release	[46]
	Biodegradable	Prolongs GI retention via mucoadhesion	Enhances colon-targeted delivery	
	Enhances mechanical stability			
Acrylic Acid (AA)	pH-sensitive monomer	Non-ionized (low pH, stomach)	Controls drug release via pH-dependent swelling	[47]

Continued on next page

Table 2.1: Polymers Used for Hydrogel Preparation (Continued from Previous Page)

Polymers Used	Properties	Mechanism of pH-Responsiveness	Findings/Applications	Reference
Carboxyl group ionization	- Ionized (high pH, colon), causing swelling			
CAP-Pectin Hybrid Hydrogels	Combines synthetic & natural polymers	CAP prevents gastric release	Improved colon-targeting efficiency	[48]
	pH-responsive degradation	Pectin swells in the colon	Decrease burst release	
Guar Gum-MAA Hydrogels	pH- and enzyme-responsive	MAA ionization at high pH	- Sustained drug release in the colon	[49]
	Higher swelling at colonic pH	Guar gum provides mucoadhesion	- Enhanced bioavailability	
Dual-Crosslinked (Physical/Chemical) Hydrogels	Pectin-CAP-MAA network	pH-dependent swelling	Enhanced drug retention in the colon	[50]
	Improved mechanical strength	Enzyme-triggered degradation	Reduced systemic side effects	

2.5 Overview of Existing Formulations

Hydrogels can be made from natural polymers, synthetic polymers, or a combination of both. These are mainly derived from plants or animals, and thus, are less likely to cause adverse reactions in the body [51]. Research approaches to studying colorectal cancer are evolving and will continue to advance with increased collaboration between researchers in the laboratory and clinicians [52], who can then apply these laboratory findings to patient management. Some possible existing areas of research on hydrogels are discussed in more detail in Table 2.2 [53].

While alginate/guar gum interpenetrating networks show pH dependent swelling, they do not retain drugs well in acidic media, which compromises gastric protection necessitating additional stabilization strategies. Although metallic crosslinkers are useful for maintaining drug release, nanocomposite hydrogels that use these crosslinkers present biocompatibility issues because of the possibility of cytotoxicity from leaching inorganic species.

Cellulose acetate phthalate-based hydrogels enable pH-triggered release but fail to achieve sufficient mucoadhesion for prolonged colonic retention, limiting their therapeutic efficacy. Alternative approaches, such as graft copolymer-based networks, offer controlled release kinetics but rely on complex synthesis routes involving cytotoxic initiators or harsh reaction conditions, hindering clinical translation.

To bridge these gaps, an ideal delivery platform must simultaneously fulfill three key criteria:

(i) robust acid resistance to prevent premature drug release in the stomach, enabled by pH-responsive polymers with high crosslinking density or dynamic shielding mechanisms;

(ii) strong mucoadhesive performance, achievable through bioinspired polymer designs that enhance interactions with colonic mucosa; and

(iii) scalable, biocompatible fabrication using GRAS (Generally Recognized as Safe) materials or aqueous-based processing.

Table 2.2: Overview of Existing Formulations

Sr.	Formulation	Type	Method of Formulation	Major Polymers	Limitations	Reference
1	pH-responsive hydrogels for delivery of capecitabine	pH-sensitive hydrogel	Free radical polymerization	Tamarind gum, β-cyclodextrin, poly (methacrylic acid)	Limited in vivo tumor model validation	[54]
2	Capecitabine-loaded nanocomposite hydrogel against murine 4T1 Breast cancer cells	Nano-composite	Crosslinking (N, N' MBAAm)	PVA, clay nanoparticles	Further biocompatibility testing of crosslinkers is required	[55]
3	IPN hydrogel microspheres	Interpenetrating network hydrogel	Emulsion crosslinking	Chitosan, poly ethylene oxide -g- acrylamide	Need for further improvement because the burst release was observed.	[56]
4	Control Delivery of capecitabine through Smart co-polymeric hydrogels	pH-sensitive copolymer hydrogel	Free radical polymerization (FRP)	Poly (acrylamide-co-acrylic acid)	Premature release at gastric pH due to high swelling.	[57]

Table 2.2: Overview of Existing Formulations (continued)

Sr.	Formulation	Type	Method of Formulation	Major Polymers	Limitations	Reference
5	IPN Mucoadhesive hydrogel beads	hydrogel beads	Ionotropic gelation Method	Sodium alginate, Gellan gum, HPMC.	Variable floating time, need stability study and improvement	[58]
6	pH-responsive hydrogel for controlled delivery	Grafted co-polymer hydrogel	FRP (Free radical polymerization)	Tamarind gum, β-cyclodextrin	High synthetic complexity, scalability issues	[59]
7	Quince seed mucilage, β-CD, Mmt-Na+ hydrogel for controlled delivery	pH-sensitive Nanocomposite hydrogel	Crosslinking	Quince seed mucilage, β-CD, montmorillonite.	mechanical strength limited	[60]

Table 2.2: Overview of Existing Formulations (continued)

Sr.	Formulation	Type	Method of Formulation	Major Polymers	Limitations	Reference
8	Tamarind gum, β-CD-co-poly(MAA) hydrogel for control delivery	Grafted pH-responsive hydrogel	Free radical polymerization	Tamarind gum, β-Cyclo-dextran, MAA	Not suitable for long-term therapy because of Potential mucosal irritation	[61]
9	Thermo-reversible hydrogel for delivery of capecitabine	Thermosensitive hydrogel	Physical crosslinking	Poloxamer, HPMC	Drug loading efficiency is low and needs improvement, gelation temperature sensitivity of gelation	[62]
10	Chitosan/agarose-g-poly-(MAA) hydrogel	pH-responsive polymeric blend	Copolymerization	Chitosan, agarose, MAA	Structural instability due to a large swelling ratio	[63]

2.6 Bridging the Gap: Natural and Synthetic Hybrid Hydrogels

Hydrogels can be derived from both natural and synthetic sources. Natural polymers, such as chitosan, pectin, alginate, and guar gum, are derived from both flora and fauna. These substances are biocompatible, non-harmful, and metabolizable, and even adhere decently to the walls of the intestine, helping to retain the medication at the target site [64]. On the other hand, natural polymers tend to be weak and do not possess sufficient mechanical strength to carry out their intended purpose for a sustained period. Furthermore, their properties can change based on their origin [65]. The labs manufacture polyacrylic acid and polyethylene glycol, which are types of synthetic polymers. These materials are strong and stable, and their design can be modified to regulate the speed of drug release [66].

Natural or synthetic polymers and copolymers that possess ionizable groups are possible pH-sensitive carriers to deliver drugs site-specifically [67]. Polymers for oral colon-targeting systems can work as the hydrophobic barrier coatings of biodegradable preparations [68]. However, there are concerns regarding their safety in large quantities, and their byproducts can be harmful at times. Furthermore, synthetic materials may not be amenable to human tissues, hence lowering their efficiency [69]. The advantages of the use of pH-sensitive materials in formulations are mostly unmatched by known techniques based on conventional production technologies [70].

To address these challenges, researchers are designing hybrid hydrogels made of both natural and synthetic parts. These hydrogels offer advantages from both sides: the natural portion is biocompatible and biodegradable, whereas the synthetic portion adds structural integrity and control. Such hybrid materials can improve safety and effectiveness for controlled drug delivery systems. Some recent studies highlighted the advantages of hybrid hydrogels for targeted delivery of drugs to the colon. One example is the combination of chitosan, a natural polymer, with Eudragit, a synthetic polymer which gellifies only at elevated pH values,

thus suitable for use in colon-targeting. The systems exhibited better stability and reduced premature leakage while maintaining a sufficiently controlled drug release profile. While these findings are encouraging, there are still many unanswered questions. Patients may have inflamed tissues, varying pH levels, or altered gut bacteria, all of which can impact the behavior of the hydrogel [71]. This is the gap we intend to fill by fabricating a novel pH-responsive hybrid hydrogel based on safe, inexpensive, and workable materials. It will also be evaluated for the ability to transport and release cancer drugs when and where they are needed. If successful, this approach may lead to better treatment outcomes, lower side effects, and improved quality of life for patients with colorectal cancer [72].

2.7 Hydrogels: Properties and Types

Hydrogels are physically or chemically crosslinked polymer networks that can retain a significant amount of water, up to thousands of times their dry weight, due to their interconnected three-dimensional structure [73]. A key requirement for hydrogels used in medical applications involves exhibiting mechanical strength and maintaining their three-dimensional structure.

In the past few decades, different types of hydrogels have been introduced, and several strategies for their development have been attempted [50]. Hydrogels can be broadly classified into two categories: natural origin hydrogels that include protein, polysaccharide, or polypeptide-based hydrogels, and synthetic origin hydrogels that include synthetic polymers or protein-synthetic hybrid hydrogels [74].

The different types of hydrogels' chemical composition and structural characteristics are critical to providing different functions. For instance, the swelling behavior, biodegradability, and mechanical properties of hydrogels are dictated by their formulation, and these are impacting factors for their possible use in drug delivery systems [75]. Hence, understanding the composition of hydrogels will provide a strong foundation for developing hydrogels tailored for specific therapeutic delivery systems [76].

Whether in solution or crosslinked form, the properties of a hydrogel are primarily determined by its chemical composition. Aqueous solutions containing very low concentrations of hydrogels are used to gain insight into the nature of hydrogels in unswollen and swollen states [77]. The swelling ratio of hydrogels can be manipulated by varying the proportion of hydrophilic versus hydrophobic groups in their structure. The ratio of hydrophilic to hydrophobic moieties can also provide a regulatory mechanism for controlling mesh size in the hydrogel network following its crosslinking [78].

In this context, hydrophilic units can be varied to dominate in the hydrogel networks, resulting in a porous microstructure. In contrast, a lower proportion of hydrophilic functionality may result in a hydrophobic network, which can thereby restrict water within a hydrogel matrix [79]. In particular, the mechanical strength of hydrogels can be widely tuned by changing the hydrogel mesh size or density of the network, which is mediated by altering molecular weights and crosslinking densities.

It is worthwhile to mention here that, unlike synthetic polymers, natural hydrogels have the distinctive advantage of having a degree of biodegradability. Additionally, other synthetic monomer units have been synthesized to form a variety of biodegradable, responsive hydrogels, illustrating the potential of hydrogels for use in future generations of drug delivery technologies [80].

2.8 Structural Characteristics

Hydrogels, specifically crosslinked polymer networks containing large quantities of water, possess a range of structural and morphological properties that contribute to their unique and highly functional behaviors [81]. This structural framework exists at various scale levels, with network architecture and crosslinking density, porosity, and agglomeration of polymer chains and precipitates impacting both the mechanism and profile of drug release [82]. The creation of hydrogel beads for drug delivery technologies can lead to particles with unique sizes and shapes, resulting

in interactions with biological tissues that endow them with specific properties. For example, investigating loading and release by hydrogel carriers of complementary shapes and sizes might result in a better understanding of inter-particle relationships with potential relevance to the transport mechanism [83].

The crosslinked nature of hydrogels can dictate the areas of maximum swelling within the hydrogel network. This influences the rate of drug release observed, as regions of increased swelling behave most similarly to mucous swelling. Lightly and highly crosslinked formulations usually display a shallow swelling edge and central swelling, respectively

[84]. Furthermore, the mechanism of network swelling owes much to the bond architecture within the network, with networks of hydrogen bonding leading to synergistic contract-swell regions. The capability of hydrogels to be porous affords them specific responsive properties that aid in their application as drug delivery vehicles [85]. Porosity and pore size dictate the overall surface area of the network, whereas pore volume and tortuosity will impact the rate at which a drug can be diffused out of a loaded hydrogel [86].

Many of the properties of hydrogels can be modified, offering a wide range of design principles to enhance performance in a variety of applications, including drug delivery [87]. Over the last decade, micro- and nanoparticles modified with an abundance of sophisticated morphologies have been the focus of extensive research. The compositional and structural design of hydrogels through selection of processing conditions permits control over their size and shape, as well as through post-fabrication processing [88]. Hollow structures with tailorable dimensions can also be achieved using template-based methods. The importance of hydrogel bead stability, burst release minimization, and the influence of gel strength on release have been studied extensively. It is essential for gel stability testing in release studies to make direct measurements of swelling behavior and mechanical properties as part of physiological behavior analysis [65].

As such, several of the tissue-engineering studies report on some determination of structural properties, as optimization of a range of structural factors may result

in overall better in vivo performance, including investigations into zwitter-ionic networks [89]. Adequate structural characterization of hydrogels was seen as not only crucial throughout the development process, to enable the formulation of weak pH networks, but also an essential factor in mechanistic release studies, where network architecture must be established in order to mechanistically account for release kinetics. The importance of hydrogel architectures whether particles, amorphous gels, or otherwise when pairing controlled porous morphologies and natural pro-chondroitin cationic glycosaminoglycans that bear negatively charged sulfate groups was also demonstrated [90].

Hydrogels have been employed in a broad range of applications and have demonstrated substantial promise in the development of new drug delivery systems. Hydrogel applications in drug delivery are frequently classified based on desired outcomes such as controlled drug release, targeted drug delivery, or the ability to combine imaging and therapy [91]. Drug-loaded hydrogels have found clinical applications, with numerous others in different stages of clinical trials for various diseases, thus underscoring their potential as drug depots [92]

Chapter 3

Materials and Methods

3.1 Materials

Capecitabine (CT) has been generously gifted by Shandong Linix Pharmaceutical Co., Ltd., China. Cellulose acetate phthalate, pectin, guar gum, and acrylic acid were sourced from Sigma-Aldrich, Germany. N, N'-methylene bis-acrylamide (MBA) and ammonium persulfate (APS) were sourced from Merck, Germany. For the preparation of simulated gastrointestinal fluids, hydrochloric acid (HCl) was purchased from Merck Marker Co. Ltd. For the simulated intestinal fluid preparation, sodium phosphate, monobasic (KH_2PO_4) and sodium hydroxide ($NaOH$) were obtained from Sigma-Aldrich, Germany. The ethanol (C_2H_5OH) used for solubilizing Capecitabine was obtained from Riedel-de Haen, Germany.Fresh distilled water was prepared using a water distillation assembly located in the Faculty of Pharmacy at Capital University of Science and Technology (CUST).

3.2 Method

Guar gum and pectin were dissolved in 50 mL of distilled water under continuous stirring at 500 rpm and subsequent heating at 50°C for better hydration and uniform swelling. For uniformity, the dispersion was kept under stirring at 600 rpm

for 30 minutes. Cellulose acetate phthalate (CAP), being water-insoluble, was dissolved separately in 10 mL of ethanol by magnetic stirring at 40°C until dissolution. The CAP solution was then slowly added into the hydration polymer dispersion under continuous stirring to prevent precipitation and ensure uniform distribution. Acrylic acid (AA) was added slowly into the polymer blend while stirring at 55°C for proper interaction with the polymeric backbone. $N, N-$methylene bisacrylamide (MBA), being the crosslinking agent, and ammonium persulfate (APS), as the free radical initiator, were dissolved separately in 5 mL of distilled water and added dropwise into the reaction medium under constant stirring at 700 rpm. The reaction medium was stirred at 60°C in a nitrogen atmosphere to prevent oxygen inhibition of the radical polymerization. The reaction mixture was refluxed at 70°C for 4–5 hours to provide a complete polymerization and stable hydrogel network. Gelation was indicated by the increase in viscosity over time. Upon polymerization, the hydrogel was left to cool at room temperature and purified by repeated washing using distilled water and 70% ethanol for the removal of unreacted monomers and other impurities. The purified hydrogel was freeze-dried. The hydrogel obtained upon drying was stored in a desiccator under vacuum awaiting further characterization [61]. The scheme of formulation, different concentrations of guar gum, pectin, CAP, AA, MBA, and APS, is shown in Table 3.1. A schematic representation of the process of hydrogel preparation is shown in Figure 3.1.

Table 3.1: Proposed Formulation Scheme for Hydrogel with Varying Concentrations of Guar Gum, Pectin, CAP, Acrylic Acid (AA), MBA, and APS

Formulation Code	**Guar gum (g)**	**Pectin (g)**	**CAP (g)**	**AA (g)**	**MBA (g)**	**APS (g)**
F1	0.5	1	0.25	10	0.4	0.2
F2	1.0	1	0.25	10	0.4	0.2
F3	1.5	1	0.25	10	0.4	0.2
F4	0.5	2	0.25	10	0.4	0.2
F5	0.5	3	0.25	10	0.4	0.2
F6	0.5	1	0.5	10	0.4	0.2
F7	0.5	1	0.75	10	0.4	0.2
F8	0.5	1	0.25	13	0.4	0.2
F9	0.5	1	0.25	16	0.4	0.2
F10	0.5	1	0.25	10	0.6	0.2
F11	0.5	1	0.25	10	0.8	0.2

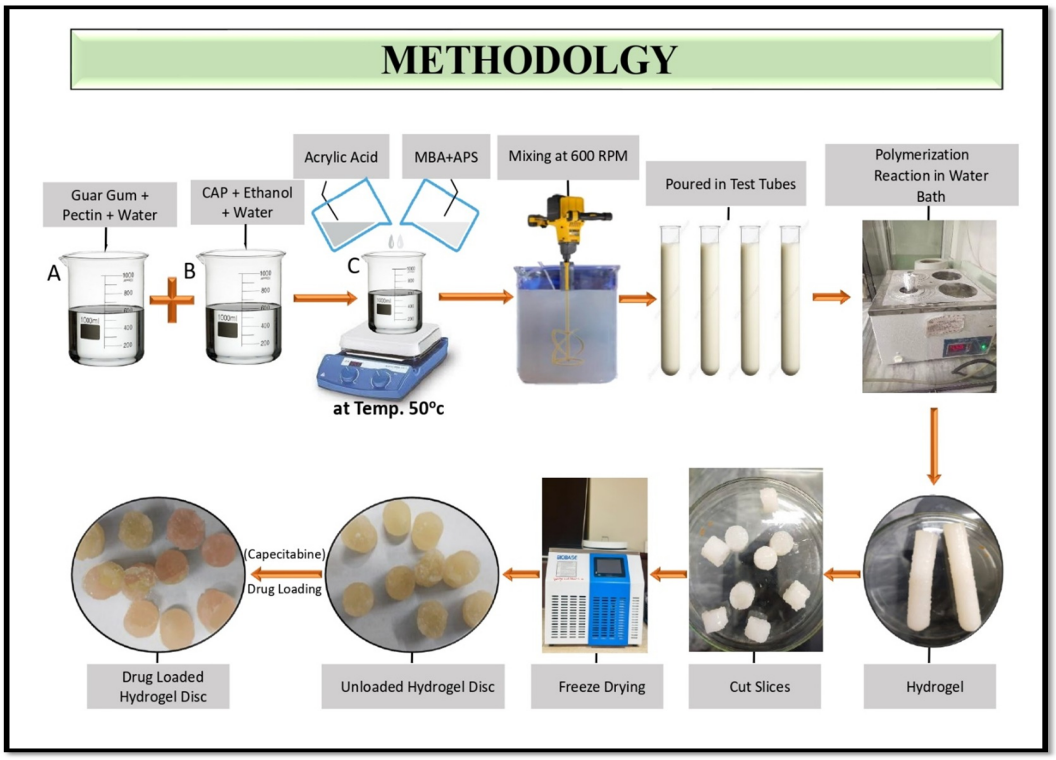

FIGURE 3.1: Schematic Representation of Hydrogel Preparation and Drug Loading Process

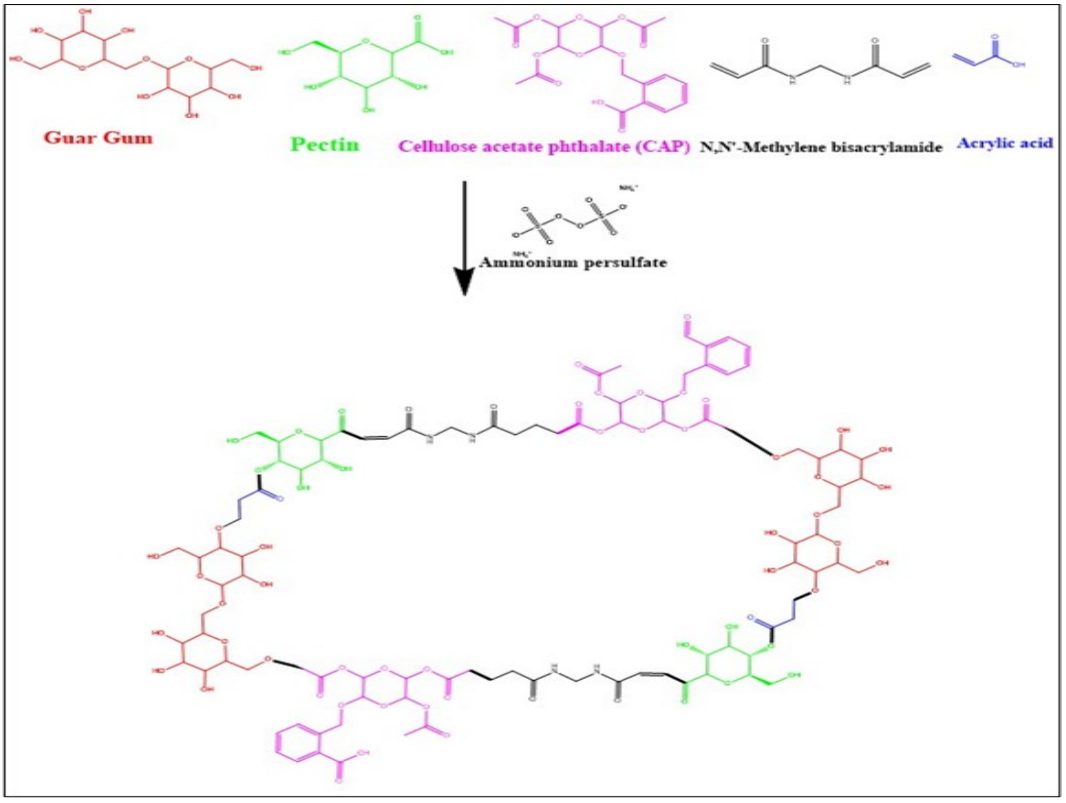

FIGURE 3.2: Structural Representation of a Crosslinked Hydrogel Network Incorporating Guar Gum, Pectin, and CA

3.3 Drug Loading

To assess drug loading under various pH settings, hydrogel discs (8.00 ± 0.05 mm diameter, 2.00 ± 0.03 mm thickness, 0.87 ± 0.02 g, n = 3) were immersed in capecitabine solution (1.0% w/v) prepared separately in simulated gastric fluid (pH 1.2) and phosphate buffer (pH 7.4). Following loading, the discs were processed in the following order: (i) washed three times for 30-second in 10 mL deionized water to eliminate drug that had adhered to the surface; (ii) blotting between Whatman® Grade 1 filter papers; and (iii) drying in a lyophilizer for 48 hours at vacuum conditions (-55°C, 0.01 mbar) to ensure complete removal of moisture and structural stabilization [93]. For additional analysis, the dried discs were stored in vacuum desiccators at 25°C and less than 10% relative humidity.

3.4 Drug Entrapment Efficiency

Encapsulation Efficiency (EE%), in vitro drug release, and swelling studies were conducted using standardized protocols to ensure experimental reproducibility. Hydrogel discs with consistent dimensions (8.00 ± 0.05 mm in diameter and 2.00 ± 0.03 mm in thickness) were prepared for all studies. A digital caliper was used to confirm dimensional accuracy. Using a calibrated analytical balance, a standard disc weight of 0.87 ± 0.02 g (n = 3 batches) was used to ensure uniformity across all experimental groups. Only discs meeting the predefined dimensional requirements were employed for subsequent evaluations.

Drug Entrapment Efficiency (DEE) was calculated by grinding drug-loaded hydrogels of a standard weight in a mortar and pestle. The ground hydrogels were transferred to 100 mL of 0.2 M phosphate buffer solution at pH 7.4 for 24 hours. Sonication will then be performed for 20 minutes for CT extraction. Polymer debris was discarded by centrifugation at 300 rpm. Fresh solvent was used for the removal of any drug attached to the polymeric debris [94]. Clear supernatant was measured for Capecitabine content using a UV-visible spectrophotometer with a

λmax of 330 nm. The Drug Entrapment Efficiency (DEE) is calculated based on the formula as indicated in equation 1:

$$\%\text{DEE} = \left(\frac{\text{Amount of drug entrapped}}{\text{Total amount of drug initially used}}\right) \times 100 \tag{3.1}$$

3.5 In Vitro Drug Release Study and Drug Release Kinetics

Dissolution profiles were assessed to evaluate the release behavior of capecitabine (CT) from the prepared hydrogels using the United States Pharmacopeia (USP) Dissolution Apparatus Type II. A dissolution medium volume of 900 mL—simulated gastric fluid (SGF) at pH 1.2 and simulated intestinal fluid (SIF) at pH 7.4—was maintained at 37 ± 0.5 °C to mimic physiological conditions.

To assess the release of CT from the hydrogels, dissolution profiles were evaluated using USP Method II with a total of 900 mL of dissolution media at 37 ± 0.5 °C. Body fluid conditions were simulated. For proper stirring, the paddle was set to 50 rpm. Gastrointestinal conditions were simulated using SGF with 1.2 pH and SIF with 7.4 pH. Samples were filtered, and do not forget to record the extraction yield. Samples of the dissolution media were withdrawn at predetermined time points—0.5, 1, 1.5, 2, 3, 4, 6, 8, 10, 12, 14, 16, 18, 20, 22, and 24 hours—and analysed quantitatively.

CT was analysed with UV spectroscopy below 330 nm, where its maximum absorbance peaks. During attendance at each sample withdrawal, fresh buffer was added to maintain sink conditions throughout the entire assay. Thus ensuring a continuity within the testing period [95].

Various mathematical models of the cumulative drug release over time were applied to investigate the Villagio hydrogel release kinetics. The primary focus was on zero order and first order models, Higuci, Hixson-Crowell as well as Korsmeter Peppas

Model. The best fit was determined from the correlation coefficients (R^2) along with several other statistical parameters providing a descriptive understanding of the drug release getaway released from the hydrogel system [96].

3.6 Swelling Studies

The initial weight (W_0)of the dry hydrogel samples was recorded as 0.87 g ± 0.02 g. The samples were then placed in a reservoir where they could not dry out, provided there was sufficient volume to prevent premature drying, and allowed to swell at controlled time intervals (1 hour, 2 hours, and 24 hours). After the desired time had passed, the samples were removed from the fluid, patted with filter paper to remove excess moisture, and weighed again to measure the swollen hydrogel mass (W_1) using a calibrated balance [97]. The swelling ratio (q) was calculated using the following formula as indicated in equation 2 :

$$q = \left(\frac{W_1 - W_0}{W_0} \right) \times 100 \tag{3.2}$$

Where,

W1 = Weight of swollen hydrogel

W0 = Weight of the dry hydrogel

3.7 Fourier Transform Infrared Spectroscopy

Fourier-transform infrared (FTIR) spectroscopy was conducted with an FTIR spectrometer equipped with attenuated total reflectance (ATR) technology.

Sample preparation for analysis will consist of carefully blending the sample with potassium bromide (KBr) in a ratio of 1:99 and grinding cautiously to ensure uniformity. The powder mixture will subsequently be compressed for 2 minutes

at a pressure of 5 tons to create translucent KBr discs of a diameter of around 13 mm. Spectra were taken in the range of wavenumber from 4,000 to 400 cm^1, and data acquisition and processing were achieved with OPUS software [98].

3.8 Scanning Electron Microscopy

The surface morphology and internal structure of the hydrogels synthesized were analyzed using scanning electron microscopy (SEM). The hydrogel samples were freeze-dried before the imaging process to remove any residual moisture and preserve the integrity of the three-dimensional network structure. The dried samples were sputter-coated with a thin gold film to provide surface conductivity and reduce charging effects under the electron beam. The coated hydrogels were mounted on aluminum stubs using conductive adhesive tape, and SEM images were taken at different magnifications for surface topography characterization [99].

3.9 Diffraction Scanning Calorimetry

The thermal stability and phase transitions of pure capecitabine and capecitabine-loaded hydrogels were analyzed using differential scanning calorimetry (DSC). For this, around 5–10 mg of each sample was accurately weighed and loaded into standard aluminum DSC pans. DSC scans were recorded within the temperature range of 30°C to 300°C at a controlled heating rate of 10°C/min under a continuous flow of nitrogen gas (50 mL/min) to establish an inert atmosphere and avoid oxidative degradation. The equipment will record the heat flow concerning any endothermic or exothermic process, such as melting, crystallization, or glass transition, that is accompanied by an increase in temperature [100]

3.10 Acute Oral Toxicity Study

The acute oral toxicity study was conducted at the Faculty of Pharmacy, Capital University of Science and Technology (CUST), Islamabad, Pakistan, in compliance

with OECD Guideline 423. Ten healthy adult female albino Wistar mice (9–10 weeks old; mean weight 21 ± 2 g) were obtained from the Animal Facility Center of CUST.

The animals were housed under controlled environmental conditions (temperature: 25 ± 2°C; relative humidity: 65 ± 5%; 12-hour light/dark cycle) with ad libitum access to water and a standardized diet.

Female mice were selected for their heightened sensitivity in toxicological assessments. The mice were acclimatized for 7 days prior to dosing and randomly divided into two groups ($n = 5/group$).

Clinical observations, including behavioral changes, food/water intake, and physiological parameters, were recorded for 14 days post-administration. This experiment also followed the Guide for the Care and Use of Laboratory Animals and the Animal Welfare Act [100]. The Pharmacy Research Ethics Committee, Faculty of Pharmacy, CUST, also approved (REC/FoP/F2024/02) the study protocol.

3.11 Dose Preparation and Administration

The Capecitabine (CT) hydrogel formulation having maximum drug loading efficiency and optimum cumulative release profile was selected to conduct the acute oral toxicity test. The OECD 423 Guidelines, namely the fixed-dose procedure for the determination of acute oral toxicity, were used to conduct the test.

Group A (Control Group): Given 0.9% normal saline in the dose volume of 1 mL/100 g body weight orally through gavage.

Group B (Treatment Group) administered the optimized hydrogel formulation (5 g/kg body weight) via oral gavage. To maintain a safe dosing volume, the 5 g/kg dose was divided into three equal fractions, administered at 30-minute intervals. The hydrogel was suspended in normal saline to achieve the target dosing volume of 1 mL/100 g body weight according to OECD guidelines [100].

3.12 Clinical Observations

All animals were observed individually after dosing, with particular attention given to the first four hours, followed by daily observations for 14 days. Clinical observations included physical alterations, such as changes in the skin, fur, mucous membranes, and eyes.

Changes in behavior were observed, like episodes of salivation, tremors, diarrhea, sleep abnormalities, and coma. Neurological effects were also recorded, especially stereotypic acts like repeated grooming, repeated circling, and posture and gait alterations.

Food and water intake were observed daily, measured in grams per animal per day and milliliters per day, respectively.

3.13 Biochemical and Hematological Test

On day 15, the animals were anesthetized using ketamine (100 mg/kg body weight, intraperitoneally) in combination with xylazine (10 mg/kg, intraperitoneally) and then euthanized via cervical decapitation. Blood samples were collected through cardiac puncture from the posterior vena cava and stored in EDTA-coated tubes for hematological analysis [101].

3.14 Histopathological Examination

Post-sacrifice, vital organs (heart, liver, kidneys, spleen, intestine, and stomach) were carefully excised, flushed with ice-cold saline, and weighed. A gross examination was conducted to detect any abnormalities or lesions.

The organs were then fixed in 10% formaldehyde solution for 48 hours, embedded in molten paraffin wax, and sectioned into 5 µm slices for hematoxylin and eosin (H&E) staining to assess histopathological changes.

3.15 Statistical Analysis

All data were presented as mean values with standard deviation. Statistical analysis was performed using SPSS® software. A one-way analysis of variance (ANOVA) was applied for comparisons involving more than two groups, while Student's t-test was used for direct comparisons between two groups. A significance level of $P < 0.05$ was used to determine statistical significance.

Chapter 4

Results and Discussion

4.1 Encapsulation Efficiency

The encapsulation efficiency (EE%) of different hydrogel formulations was evaluated at pH 1.2 and pH 7.4 to assess drug retention and potential release behavior under acidic and physiological conditions. The results are summarized in Table 4.1.

Table 4.1: Encapsulation Efficiency (EE%) of Hydrogel Formulations at pH 1.2 and pH

Formulation	**EE% (pH 1.2) Mean ± SEM**	**EE% (pH 7.4) Mean ± SEM**
F1	54.000 ± 0.630	80.000 ± 0.710
F2	55.920 ± 0.730	81.000 ± 0.730
F3	58.270 ± 0.820	82.000 ± 0.720
F4	70.000 ± 0.600	95.000 ± 0.550
F5	62.000 ± 0.850	86.490 ± 0.940
F6	49.380 ± 0.540	76.120 ± 0.810
F7	45.400 ± 1.040	73.290 ± 0.570
F8	60.000 ± 0.870	84.000 ± 0.580
F9	67.610 ± 0.730	89.740 ± 0.650
F10	64.740 ± 0.940	86.740 ± 0.450
F11	40.360 ± 0.630	71.060 ± 0.700

Different formulations had different levels of drug retention, according to the EE% data. The range of EE% in SGF (pH 1.2) was 40.36% (F11) to 70.00% (F4). The maximum EE% in F4 (70.00 ± 0.60%) indicates ideal cross-linking density and polymeric interaction, which probably leads to better drug entrapment. Other formulations showed a notable EE%, suggesting relatively stable polymer networks, including F9 (67.61 ± 0.73%), F10 (64.74 ± 0.94%), and F5 (62.00 ± 0.85%). The significantly lower EE% of F6 (49.38 ± 0.54%), F7 (45.40 ± 1.04%), and F11 (40.36 ± 0.63%), on the other hand, may have resulted from less than ideal polymer ratios, decreased cross-linking, or excessive porosity that impairs drug retention in acidic environments [102]. All formulations showed an improvement in EE% at pH 7.4, which is indicative of improved drug retention and polymer stability under physiological conditions. As demonstrated by its robust network and effective drug loading, F4 once again achieved the highest EE% (95.00 ± 0.55%), outperforming other formulations by a significant margin (p ¡ 0.01, ANOVA with Tukey's post hoc test). While their values were still statistically lower than F4, other high-performing formulations were F9 (89.74 ± 0.65%), F10 (86.74 ± 0.45%), and F5 (86.49 ± 0.94%).

Possibly as a result of weak polymer–drug interactions or intrinsic structural flaws that promote premature drug diffusion, formulations F7 (73.29 ± 0.57%) and F11 (71.06 ± 0.70%) showed the lowest EE% at pH 7.4. Tukey's post hoc test validated F4's dominance ($p < 0.01$), and statistical analysis (one-way ANOVA) confirmed significant inter-formulation differences at pH 1.2 ($p < 0.05$) and pH 7.4 ($p < 0.001$) [103].

4.2 In Vitro Dissolution and Drug Release Kinetics

The in vitro release behavior of capecitabine-loaded hydrogel formulations (F1–F11) was evaluated in simulated gastric fluid (pH 1.2) and simulated intestinal fluid (pH 7.4) to simulate physiological conditions. The results are shown in Figure 4.1A,

B & C and Table 4.2. Drug release was significantly influenced by the pH of the medium and the formulation composition. Overall, a slower and limited release was observed at pH 1.2, while a faster, sustained release was evident at pH 7.4 across all formulations, indicating clear pH-sensitive behavior of the hydrogel matrix.

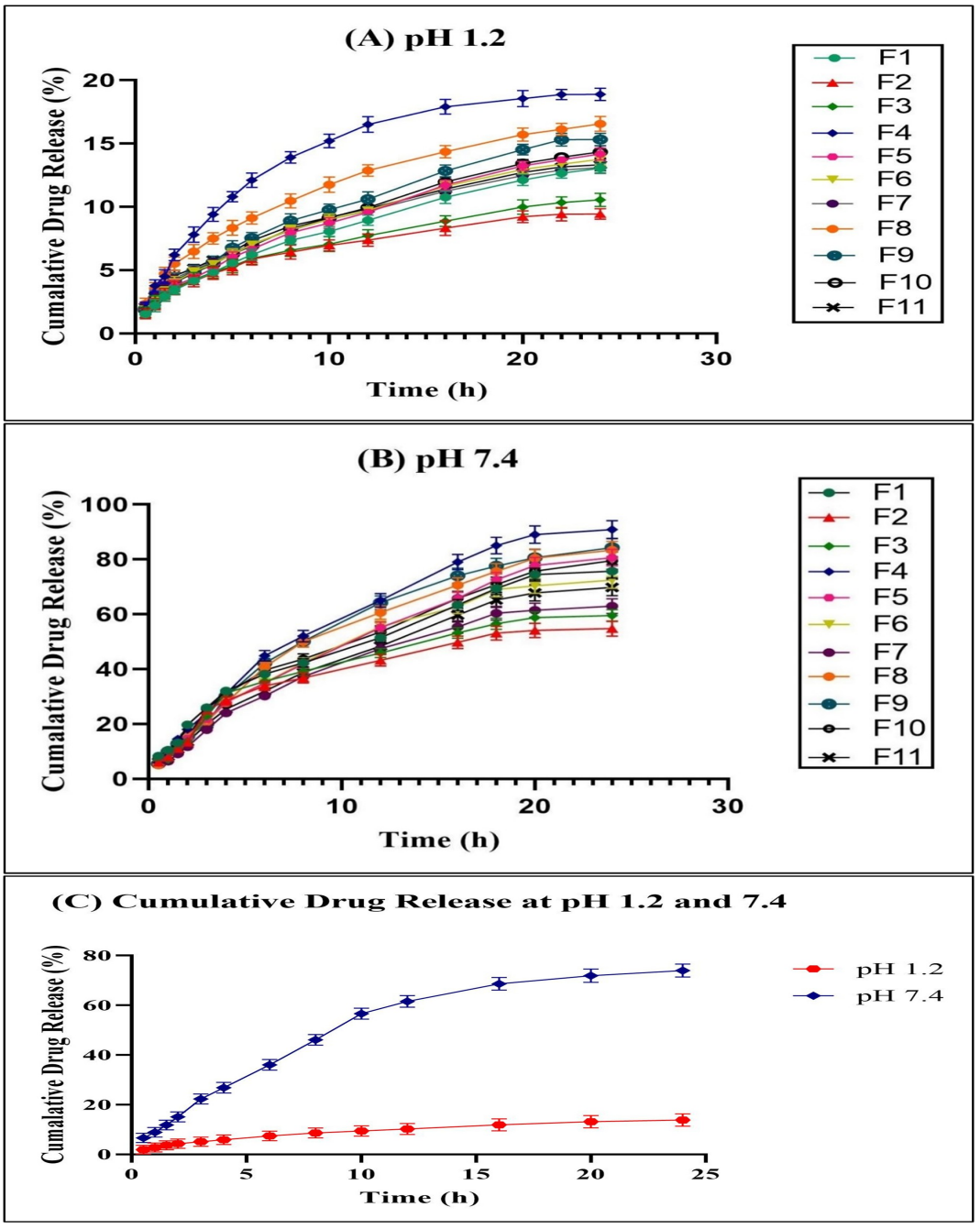

FIGURE 4.1: In Vitro drug release profiles of Capecitabine-loaded hydrogel formulations at (A) pH 1.2, (B) pH 7.4, and (C) Cumulative mean drug release at both pH 1.2 and pH 7.4. Data are presented as mean $SD(n = 3)$. Statistical significance between groups was assessed by one-way ANOVA ($p < 0.05$).

TABLE 4.2: In vitro drug release kinetics of capecitabine-loaded formulations (F1-F11) at pH 1.2 and 7.4 using Zero-Order, First-Order, Higuchi, and Korsmeyer–Peppas Models

Formulations		**Zero Order**		**First Order**		**Higuchi**		**Korsmeyer-Peppas**		
	pH	R^2	K	R^2	K	R^2	K	R^2	K	n
F1	1.2	0.969	0.697	0.768	0.116	0.995	2.525	0.996	2.411	0.530
	7.4	0.956	4.193	0.789	0.092	0.993	14.651	0.991	14.425	0.508
F2	1.2	0.931	0.600	0.670	0.113	0.978	2.327	0.978	4.393	0.167
	7.4	0.883	3.290	0.501	0.224	0.967	11.900	0.993	19.108	0.264
F3	1.2	0.949	0.608	0.699	0.115	0.989	2.437	0.988	4.223	0.213
	7.4	0.895	3.455	0.521	0.228	0.972	12.286	0.974	17.918	0.316
F4	1.2	0.874	1.280	0.594	1.158	0.967	4.381	0.965	8.711	0.158
	7.4	0.951	5.090	0.566	0.246	0.993	16.707	0.986	21.742	0.373
F5	1.2	0.970	0.760	0.760	0.122	0.994	2.720	0.995	2.676	0.514
	7.4	0.971	4.088	0.595	0.233	0.995	13.999	0.996	12.295	0.565
F6	1.2	0.960	0.739	0.721	0.125	0.995	2.844	0.994	3.653	0.371
	7.4	0.946	3.837	0.572	0.231	0.992	13.611	0.988	17.459	0.379
F7	1.2	0.906	0.624	0.669	0.129	0.990	2.978	0.983	4.250	0.312
	7.4	0.952	2.970	0.607	0.218	0.987	11.899	0.986	20.961	0.236
F8	1.2	0.930	0.952	0.634	0.145	0.988	3.715	0.988	7.417	0.150
	7.4	0.948	4.653	0.766	0.120	0.993	14.971	0.975	16.441	0.454
F9	1.2	0.807	1.030	0.605	0.141	0.923	3.390	0.878	6.792	0.137
	7.4	0.801	5.443	0.412	0.249	0.988	15.048	0.964	21.501	0.338
F10	1.2	0.968	0.767	0.735	0.126	0.995	2.870	0.996	2.924	0.494
	7.4	0.956	4.005	0.560	0.236	0.994	14.242	0.996	14.201	0.509
F11	1.2	0.936	0.744	0.677	0.130	0.989	3.019	0.988	5.379	0.204
	7.4	0.963	3.606	0.594	0.226	0.995	12.394	0.995	14.402	0.435

The protonation of carboxylic groups at pH 1.2 was responsible for the limited drug release (20–40% over 12 hours), which limited the swelling of the hydrogel. The burst release kinetics of formulation F4 (Korsmeyer–Peppas n = 0.158) indicated matrix erosion brought on by excessive swelling caused by pectin. On the other hand, F5 (3 g pectin, 0.25 g CAP) showed Fickian diffusion (n = 0.514, R2 = 0.995), which is an indicator of a stable polymeric network with controlled release controlled by concentration-driven diffusion. Ionization of functional groups promoted increased swelling at pH 7.4, which resulted in sustained drug release (70–95% over 24 hours). A combined mechanism of diffusion and polymer chain relaxation was demonstrated by F5's anomalous transport (n = 0.565, R2 = 0.996). In contrast, F4's lower pectin content (2 g) caused it to swell quickly, which led to an early release of the drug (n = 0.373), making it suboptimal for sustained delivery [104].

The encapsulation efficiency (EE%) (45.40–49.38% at pH 1.2) and release behavior (n = 0.312–0.371) of formulations with a higher CAP content (F6–F7: 0.5–0.75 g) were lower, most likely as a result of hydrophobic aggregation that compromised network stability. Similarly, higher MBA concentrations (F10–F11: 0.6–0.8 g) resulted in brittle and excessively cross-linked matrices, which decreased the EE% (40.36–64.74%) and inhibited diffusion (R2 ¡ 0.99 for Higuchi model at pH 1.2). The moderate EE% (67.61–89.74%) and poor release kinetics (n = 0.137–0.338) of F9, which contained 16 g of acrylic acid, could have been caused by non-uniform swelling behavior linked to an excessive monomer content. The Korsmeyer–Peppas model best described release kinetics across all formulations, suggesting a hybrid mechanism combining diffusion and polymer relaxation. While protonation at pH 1.2 limited porosity and restricted drug mobility, ionization at pH 7.4 mechanistically linked the pH-responsive behavior by increasing mesh size and diffusivity. The composition of the polymer was important; a higher pectin content (F4: 2 g; F5: 3 g) increased the EE% but necessitated balanced CAP loading to prevent excessive swelling. However, excessive CAP or MBA caused network instability, which decreased drug retention and control release [26]. Despite having the highest encapsulation efficiency (95.00 ± 0.55 percent at pH 7.4), Formulation F4 showed

an erosion-dominated release profile (n = 0.158), which could result in a reduced therapeutic window and early drug expulsion. Because Formulation F5 performed better across all important parameters for colon-targeted drug delivery, it was chosen as the best option.

Notably, F5 displayed a pH-dependent sustained release profile, with 86% at pH 7.4 over 24 hours. This contrasts sharply with the rapid, pH-independent release behavior of commercial capecitabine formulations such as Xeloda®. Immediate-release formulations like Xeloda® are known to exhibit rapid dissolution, releasing over 90% of the drug within 2 hours in both gastric and intestinal media.This accelerated release contributes to upper gastrointestinal absorption, often leading to dose-limiting toxicities—such as diarrhea and hand-foot syndrome—and necessitates frequent high-dose regimens ($1,250 mg/m^2$ twice daily).

In contrast, F5 controlled and pH-sensitive release behavior, governed by anomalous transport kinetics (n = 0.565), reflects a combination of Fickian diffusion and polymer matrix relaxation. This release mechanism promotes retention in the upper GI tract while allowing selective drug release in the colonic region, potentially minimizing systemic toxicity and reducing dosing frequency.

The superior performance of F5 is attributed to its rationally designed polymeric matrix. Cellulose acetate phthalate offers enteric protection, while pectin and guar gum facilitate swelling-mediated, controlled release in the colonic pH environment features absent in conventional immediate-release systems. Literature supports that such pH-responsive delivery systems can enhance therapeutic indices by 40–60% in preclinical models compared to standard oral formulations [14].

Although F5 exhibited a slightly lower encapsulation efficiency (86.49 ± 0.94%) than F4, this was offset by its significantly improved pH-responsive release characteristics, essential for effective colonic targeting. F5 is positioned as a promising candidate due to its overall performance, which includes encapsulation efficiency, swelling behavior, and release kinetics. The F5 controlled-release mechanism is further supported by the Korsmeyer–Peppas model, enhancing its potential for clinical uses targeted at lowering systemic side effects and dosing frequency [25].

4.3 Swelling Dynamics of Hydrogels

4.3.1 *Influence of Polymers, Monomers, and Crosslinking Agents on Swelling Behavior of Hydrogels*

Hydrogel swelling behavior is dictated by three key factors: (1) the hydrophilic-hydrophobic balance of polymers, (2) polymer concentration, and (3) crosslinking density.

These factors collectively regulate water absorption, network expansion, and mechanical stability. Figure 4.2 illustrates this mechanism, depicting how the hydrogel's covalently crosslinked interpenetrating network (Guar Gum, Pectin, CAP, AA, MBA) dynamically responds to pH changes:

4.3.2 *Effect of Guar Gum Content on Swelling Properties*

Hydrogel swelling is strongly influenced by the guar gum content; as the guar gum concentration rises, the swelling decreases, as shown by the trend $F1 > F2 > F3$, as shown in Figure 4.2. Through hydrogen bonding, guar gum, a polysaccharide rich in hydroxyls, improves water absorption. Because there are a lot of free hydroxyl groups that form hydrogen bonds with water and create a porous network, F1 (0.5 g guar gum) has the highest swelling index (75.49 at pH 7.4). Because polymer chain entanglements prevent solvent penetration, F2 (1.0 g guar gum) exhibits less swelling (72.16). Because too much guar gum raises crosslinking density and forms a rigid, compact network that significantly restricts water uptake, F3 (1.5 g guar gum) has the lowest swelling (65.48) [49].

This is consistent with the Flory-Rehner theory, which states that swelling capacity and free volume decrease with increasing polymer concentrations. At pH 1.2, the hydrophilic contributions of guar gum predominate, and electrostatic repulsion

is suppressed by protonating carboxyl (-COOH) groups from pectin/acrylic acid, which results in minimal swelling [46].

4.3.3 Effect of Pectin Concentration on Swelling Kinetics

The hydrogel's swelling behavior is critically controlled by the pectin concentration, as shown by the trend $F4 > F5 > F1$ at pH 7.4, as shown in Figure 4.2. Using hydrogen bonds and electrostatic interactions, pectin, a polysaccharide abundant in carboxyl (-COOH) and hydroxyl (-OH) groups, promotes hydrogel swelling. Significant water absorption is caused by electrostatic repulsion and osmotic pressure created by the ionization of carboxyl groups at pH 7.4. Because of balanced network porosity and optimal ionization, F4 (2.0 g pectin) has the highest swelling index (78.63%), allowing for effective water absorption while preserving structural integrity [104]. The dense yet responsive network effectively retains the drug in acidic conditions and facilitates controlled release in intestinal pH, which is consistent with its superior encapsulation efficiency (EE% = 70.00 ± 0.60 at pH 1.2; 95.00 ± 0.55 at pH 7.4). Because of steric hindrance and polymer chain entanglement, which restricts solvent diffusion, F5 (3.0 g pectin) shows somewhat less swelling (76.70%). Despite this, its sustained release kinetics and moderate EE% (62.00 ± 0.85 at pH 1.2; 86.49 ± 0.94 at pH 7.4) point to a stable but less porous matrix that is excellent for prolonged intestinal delivery. The lowest swelling (75.49%) and EE% (54.00 ± 0.63 at pH 1.2; 80.00 ± 0.71 at pH 7.4) are seen in F1 (1.0 g pectin), which indicates weaker drug retention and insufficient carboxyl groups for strong electrostatic repulsion [105].

4.3.4 *Effect of Cellulose Acetate Phthalate on Swelling Behavior*

Hydrogel formulations exhibit the following swelling trend: $F1 > F6 > F7$, as shown in Figure 4.2. A hydrophobic polymer with acetate and phthalate groups, CAP lowers water affinity and, consequently, swelling characteristics. Because

of the predominance of hydrophilic interactions, the swelling index at pH 7.4 is high (75.49%) at 0.25% CAP (F1). Swelling decreases to 56.43% when CAP is raised to 0.5% (F6), and water absorption remains even lower at 0.75% (F7). This supports Huggins' theory, which states that greater hydrophobicity prevents solvent diffusion. Because of CAP's natural hydrophobicity, which overrides pH effects, all formulations containing CAP show minute swelling ($< 6\%$) at pH 1.2 [106].

4.3.5 *Effect of Acrylic Acid on Swelling Behavior*

The effects of different AA contents (10%, 13%, and 16%, respectively) were examined for Formulations F1, F8, and F9. As the concentration of AA increased, the swelling index increased proportionately ($F1 : 75.49\% < F8 : 78.26\% < F9 : 80.49\%$) as shown in Figure 4.2. Ionizable -COOH groups from AA produce -COO sites when they ionize, which improves electrostatic repulsion between polymer chains and raises osmotic pressure. This promotes greater solvent uptake and helps the hydrogel network grow [45]. The findings are in line with the polyelectrolyte swelling theory, which credits increased hydrophilicity and charge density with better swelling behavior. It should be remembered, though, that excessive charge accumulation can ultimately result in counterion condensation, which lowers the swelling efficiency brought on by charge screening [47].

4.3.6 *Effect of Crosslinker on Swelling Behavior*

The hydrogels' swelling behavior displays an inverse relationship between N, N-methylene bisacrylamide (MBA) concentration, and solvent uptake, following the trend $F1 > F10 > F11$ (see Figure 4.3). By changing the crosslink density, MBA functions as a crosslinking agent that modifies the hydrogel matrix's structural integrity. Because of its moderate crosslinking, which preserves network flexibility while maintaining enough porosity for water absorption, F1 (0.4 g MBA) has the highest swelling index (75.49% at pH 7.4). The increased crosslink density in F10

(0.6 g MBA) limits the mobility of the polymer chains, lowering the swelling index to 62.04% at pH 7.4. Excessive crosslinking in F11 (0.8 g MBA) results in a stiff and compact network that severely restricts solvent penetration and slowers the swelling index to 57.62% at pH 7.4 [49]. The Flory–Rehner theory, which believes that a higher crosslink density inhibits solvent uptake by decreasing network flexibility and free volume, is supported by this inverse correlation. Because of the protonation of carboxyl (-COOH) groups (from pectin/acrylic acid) and the predominance of hydrophobic interactions (from CAP), which overcome hydrophilic contributions regardless of MBA concentration, all formulations show only modest swelling (3–6%) at pH 1.2 [107].

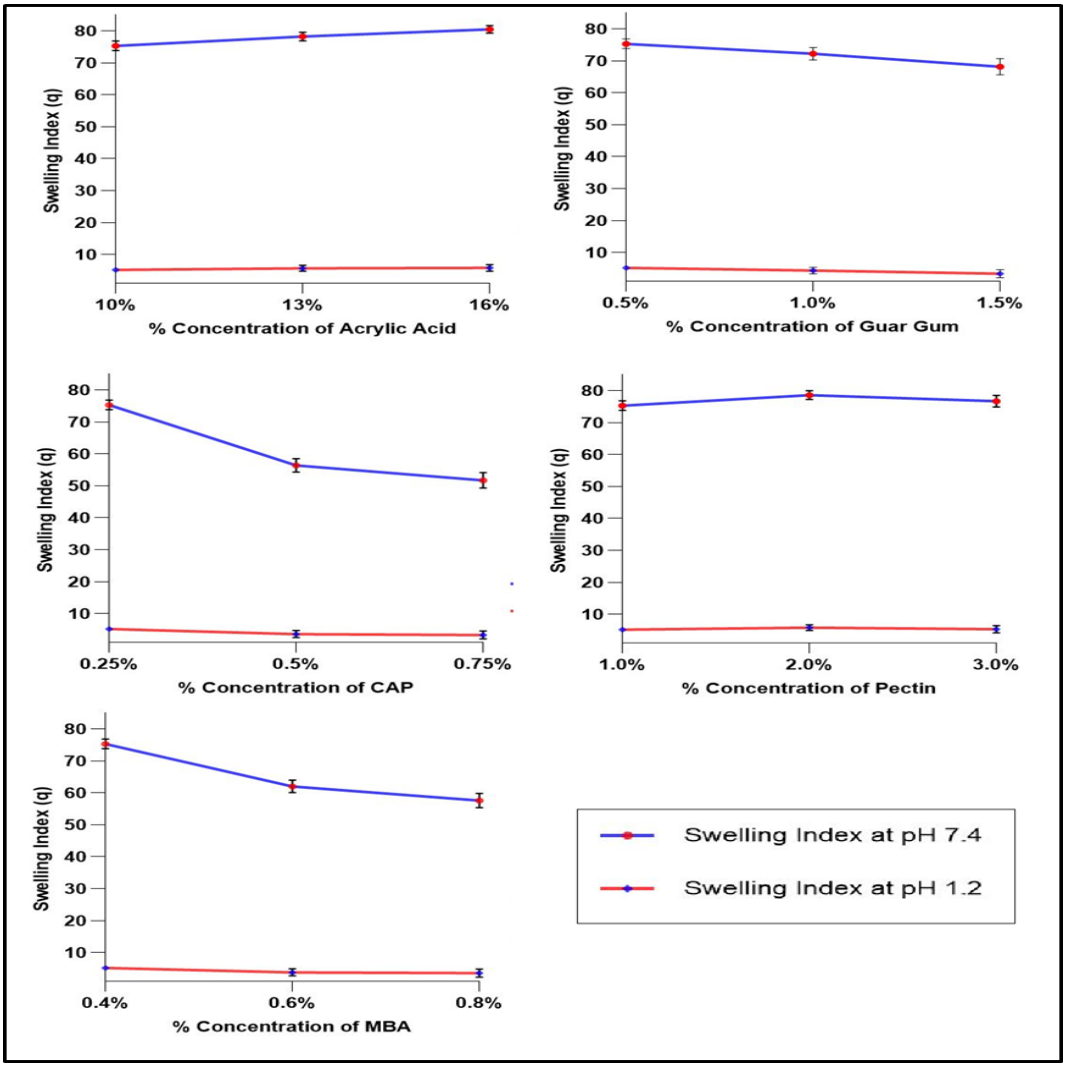

FIGURE 4.2: Effect of Acrylic Acid, Guar Gum, CAP, Pectin, and MBA on the swelling index (q) of the hydrogel formulations at pH 7.4 and pH 1.2. Values are represented as mean ± SD (n=3)

4.3.7 *Effect of pH on Swelling*

Figure 4.3 indicates how the hydrogel formulations' swelling behavior demonstrated a distinct pH dependence, confirming their suitability for pH-responsive drug delivery. Controlled by thermodynamic and kinetic principles, the pH-responsive swelling behavior of the hydrogel formulations results from a complex interaction between osmotic-driven network restructuring, solubility transitions of functional excipients, and ionization-dependent polymer chain interactions. Protonation of the carboxyl (-COOH) groups in pectin and acrylic acid (AA) in acidic media (pH 1.2) removes ionizable charges, reducing electrostatic repulsion between polymer chains and promoting intramolecular and intermolecular hydrogen bonding. The hydrophobic domains of undissolved cellulose acetate phthalate (CAP), which form a compact, glassy state below its pKa (5.5) and serve as a physical barrier to solvent permeation, further reinforce this conformational collapse. Water penetration is limited by the resulting decrease in free volume and osmotic pressure (as determined by the Gibbs free energy equation, $\Delta G = \Delta H - T\Delta S$), which results in minimal swelling indices (3.38 ± 0.25 to 5.89 ± 0.18). Together, the steric hindrance of CAP and the predominance of hydrophobic interactions stabilize the collapsed network, ensuring gastric protection [108].

At physiological pH (7.4), deprotonation of carboxyl groups generates negatively charged (-COO) moieties, inducing electrostatic repulsion that overcomes hydrogen bonding, thereby expanding the mesh size of the hydrogel network. Concurrently, CAP undergoes ionization and dissolution, transitioning from a hydrophobic glassy state to a soluble, hydrophilic phase, which eliminates steric constraints and enhances solvent accessibility.

The Donnan equilibrium effect amplifies osmotic pressure, driving rapid water influx and network relaxation. Hydrophilic components like guar gum, with its high density of hydroxyl (-OH) groups, synergize with ionized AA/pectin to form hydrated channels via bound water clusters, further augmenting swelling (51.74 ± 1.6 to 80.49 ± 0.8). Statistical modeling using regression analysis revealed a strong correlation between swelling indices and pH, with an R^2 of 0.926 and

overall significance ($p < 0.001$). One-way ANOVA followed by Tukey's post-hoc test confirmed that swelling at pH 7.4 was significantly higher than at pH 1.2 across all formulations ($p < 0.05$), in alignment with the proposed ionization-driven swelling mechanism.

Although formulation-specific deviations emerged, statistical modeling (ANOVA, R2 = 0.926, p¡0.001) validated pH as the principal variable. Through uncontrolled

electrostatic repulsion, excess pectin (F4: 2 g) or AA (F9: 16 g) broke structural coherence, resulting in non-Fickian burst release (Korsmeyer-Peppas $n < 0.4$), which is a sign of erosion-dominated kinetics. High crosslinker concentrations (F10–F11: 0.6–0.8 g MBA), on the other hand, increased crosslink density, decreased solvent diffusivity, and consequently decreased swelling (< 62.041.1).

The most optimal formulations (such as F5: 3 g pectin, 0.25 g CAP) produced a metastable balance: pH-selective swelling (76.70 ± 1.2) with Fickian diffusion, which is controlled by concentration gradients (Fick's first law), was made possible by controlled ionization and CAP dissolution, while moderate crosslinking-maintained network integrity.

Following zero-order kinetics ($R2 = 0.995$), this balance between electrostatic expansion and crosslink-imposed restraint guaranteed minimal gastric drug leakage (EE% = 62.00 ± 0.85 at pH 1.2) and sustained intestinal release (86.49 ± 0.94% EE%, n=0.565 at pH 7.4).

Using gastrointestinal pH gradients to spatially target a therapeutic release paradigm that is consistent with the observed correlation between swelling dynamics and release profiles, the pH-triggered transition from a CAP-stabilized glassy matrix to a hydrophilic, ionized network is an example of a stimuli-responsive drug delivery mechanism.

These results highlight how important it is to balance crosslink density, excipient solubility, and polymer ionization to create hydrogels with programmable pH-responsive behavior [109].

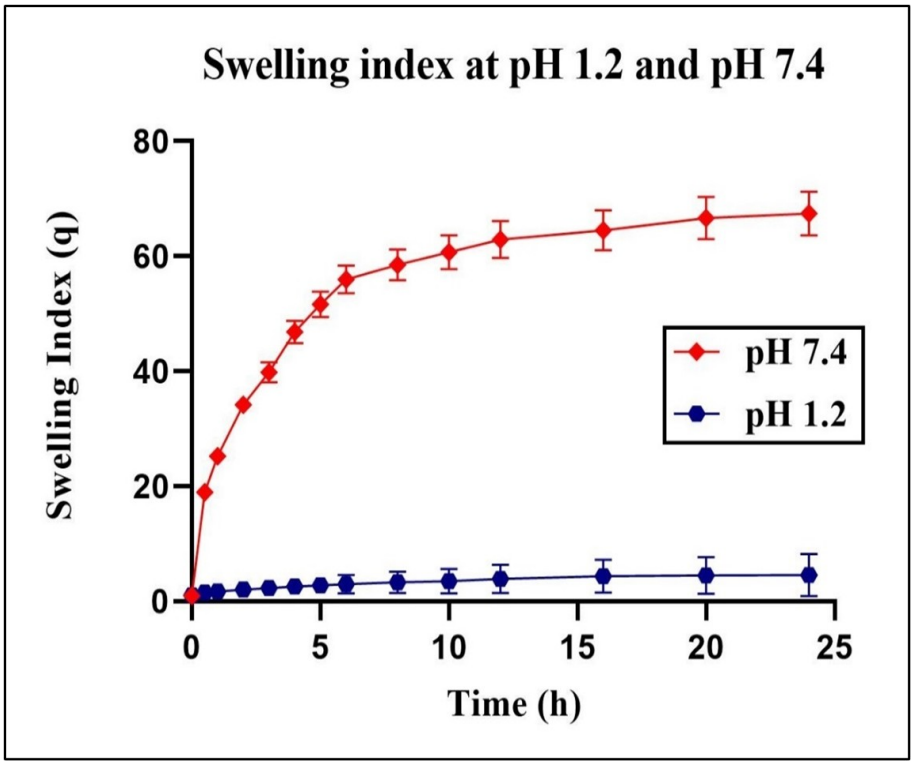

FIGURE 4.3: Swelling index of hydrogel formulations at pH 1.2 and pH 7.4 over a 24-hour period. Data are presented as mean ± SD (n= 3). Error bars represent SD. Statistical significance was determined by one-way ANOVA ($p < 0.05$) across different formulations (F1–F11)

4.4 Fourier-Transform Infrared Spectroscopy

To ensure compatibility of the structure and the drug with the excipients, the FTIR spectra of all ingredients and the final formulation was evaluated, focusing on functional group presence to confirm lipid-excipient compatibility.

The FTIR spectra corresponding to fully functionalized polymers depict that the expected constituent parts are present along with necessary reactions in the resulting polymer framework(s), which is evidenced with the optimized blend of hydrogels shown in Figure 4.4.

The presence of acrylic acid (AA) within the structure was confirmed through FTIR due to the broad O-H stretching absorption band from 3200-3400 $cm^{-}1$ along with characteristic C=O stretching of carboxyl at 1705 $cm^{-}1$.

Similar to this, the FTIR of Capecitabine (CT) revealed strong bands at 1240 $cm^{-}1$, which is C-N stretching, and at 1650 cm^{1}, which is C=O stretching of the amide group, both of which demonstrate the molecular structure of the drug.

These results demonstrate the effective incorporation of excipients in the polymeric matrix by confirming the presence of significant functional groups that are in charge of hydrogel formation and drug encapsulation [91].

To identify the structure of cellulose acetate phthalate (CAP) it was analyzed by FTIR revealing peaks at 1735 cm-1 due to the C=O stretching of the ester bond and 1160 cm-1 due to C-O-C stretching [48].

In FTIR analysis of guar gum (GG) the most prominent feature was the broad O-H stretching peak around 3400 cm-1, typical of polysaccharides.

As to N,N'- Methylenebisacrylamide (MBA), its function as a cross-linker was characterized through the noted sharp peaks at 1655 $cm^{-}1$ and 1550 cm-1 which correspond to the amide I (C=O stretching) and amide II (N-H bending) bands, respectively [49].

From the FTIR spectra of pectin (PEC) there are the well distinguished peaks at 3400 cm-1 for O-H stretching as well as 1610 $cm^{-}1$ for asymmetrical stretching of the carboxylate (-COO-) group, thus suggesting PEC is a polysaccharide [110].

The FTIR spectrum of the optimized hydrogel formulation showed absorption bands characteristic of the functional groups of all the individual components with minor shifts in wavenumber and variation in peak intensities.

The characteristic peaks of AA, MBA, and CAP were preserved, but broadening of the O-H stretching region at 3200–3400 $cm^{-}1$ and shifts in C=O stretching in 1700–1720 $cm^{-}1$ imply successful polymerization and hydrogen bonding interactions in the hydrogel matrix, implying effective encapsulation of CT in the polymeric network.

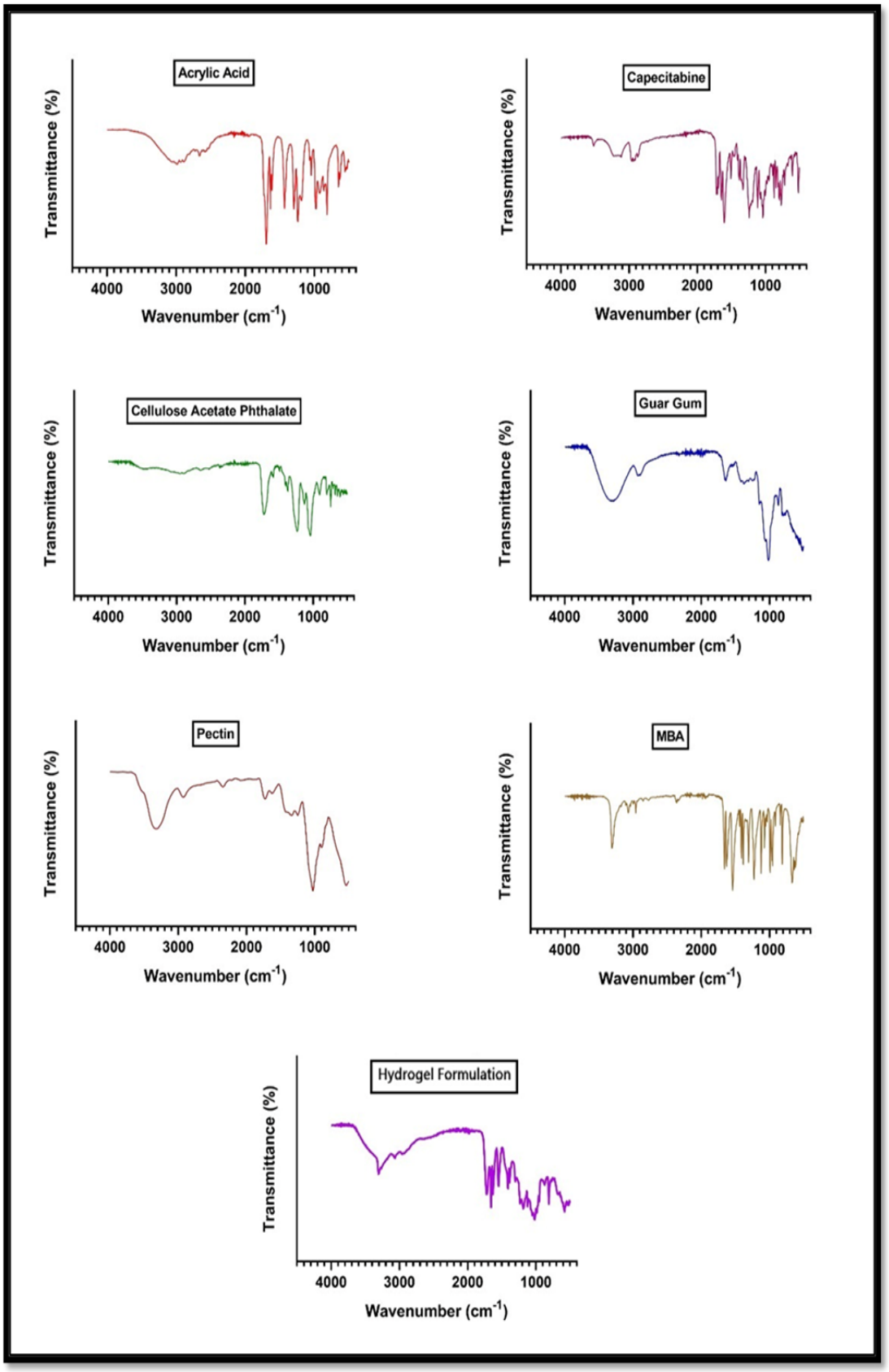

FIGURE 4.4: FTIR spectra of Capecitabine (CT), Acrylic Acid (AA), Guar Gum (GG), Cellulose Acetate Phthalate (CAP), Pectin (PEC), N, N-Methylenebisacrylamide (MBA), and optimized Hydrogel Formulation

4.5 X-ray Diffraction

An X-ray diffraction (XRD) analysis was carried out to investigate the crystalline nature of individual components and the final hydrogel system.

The PXRD spectra presented in Figure 4.5 demonstrate the distinct diffraction patterns of Capecitabine (CT), Pectin (PEC), Guar Gum (GG), and Cellulose Acetate Phthalate (CAP), indicating their semi-crystalline to crystalline nature.

In contrast, the optimized hydrogel formulation exhibited a broad, diffused halo, suggesting a significant reduction in crystallinity, which confirms successful molecular dispersion of the drug within the hydrogel matrix. This amorphization is advantageous for enhancing drug solubility and release performance.

The diffractogram of pectin (PEC) showed a sharp crystalline peak at 22.1°, thus establishing its semi-crystalline nature.

Capecitabine (CAP) showed intense and sharp diffraction peaks at 10.5°, 14.8°, 18.2°, and 22.7°, thus establishing its highly crystalline nature. XRD pattern of guar gum (GG) showed a broad halo at 18.5°, establishing its highly amorphous nature.

Cellulose acetate phthalate (CAP) showed diffraction peaks at 13.2° and 19.6°, establishing partial crystallinity [101]. The diffractogram of the final hydrogel system showed a broad and diffuse pattern, lacking the sharp diffraction peaks of CAP, establishing loss of crystallinity during hydrogel formation.

The failure of distinct crystalline reflections of CAP within the polymeric matrix establishes dispersion at the molecular level, establishing successful encapsulation. The drug conversion from crystalline to amorphous nature in the hydrogel matrix establishes enhanced solubility and dissolution behavior, essential to ensure controlled and sustained release of the drug. The overall loss of crystallinity, as established through peak broadening and reduced intensity, further establishes the formation of a crosslinked polymeric network with uniform dispersion of the drug [111].

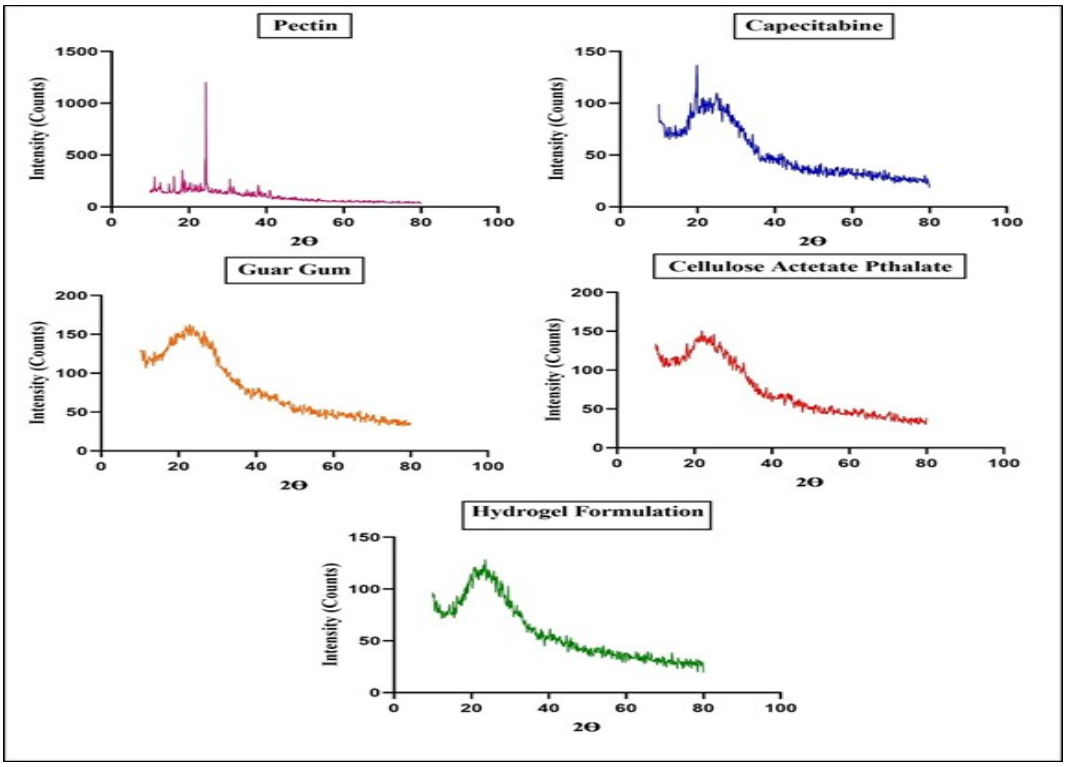

FIGURE 4.5: XRD spectra of Capecitabine (CT), Pectin (PEC), Guar Gum (GG), Cellulose Acetate Phthalate (CAP), and Optimized Hydrogel Formulation. Peak assignments: CT (10.5°, 14.8°, 18.2°, 22.7°), PEC (22.1°), GG (18.5°), CAP (13.2°, 19.6°). The hydrogel shows a diffuse pattern, confirming amorphization

4.6 Scanning Electron Microscopy

The surface morphology of the optimized Capecitabine-loaded hydrogel formulation was extensively analyzed using scanning electron microscopy (SEM) to evaluate its structural integrity, porosity, and surface characteristics, which are critical factors influencing its pharmaceutical performance. As depicted in Figure 4.6, the SEM micrographs of optimized hydrogel formulation at varying magnifications reveal a highly porous, sponge-like structure characterized by well-defined, interconnected pores distributed uniformly throughout the hydrogel matrix. This porous architecture plays a pivotal role in enhancing the water absorption and swelling behavior of the hydrogel, which are essential for its controlled drug release capabilities. The lyophilization method used in the preparation of hydrogels helps in creating an interconnected porous network.

This method enhances the surface area and porosity of the structure by leaving behind a network of voids and channels through the sublimation of ice crystals from frozen hydrogel under reduced pressure. The permeable structure of the hydrogel matrix is beneficial because it facilitates rapid penetration and diffusion of water, thus increasing swelling indices and providing multiple pathways for the controlled and sustained release of capecitabine. Furthermore, the SEM Images taken with higher magnifications show a smooth and continuous polymeric surface, which does not reveal any crystalline drug particles. This is evidence that Capecitabine was encapsulated within the hydrogel network. A controlled and consistent therapeutic effect results from the drug's evenly distributed molecular level within the polymeric matrix and prevents premature release. The lack of distinct drug crystals on the surface supports this reasoning. The hydrogel's strong and flexible structural integrity portrays its potential application in targeted and sustained drug delivery systems.The morphological characteristics seen in the SEM analysis validate the successful creation of a hydrogel system with the appropriate porosity and encapsulation efficiency, confirming its appropriateness for use in pharmaceutical applications meant to improve Capecitabine's bioavailability and therapeutic efficacy [99].

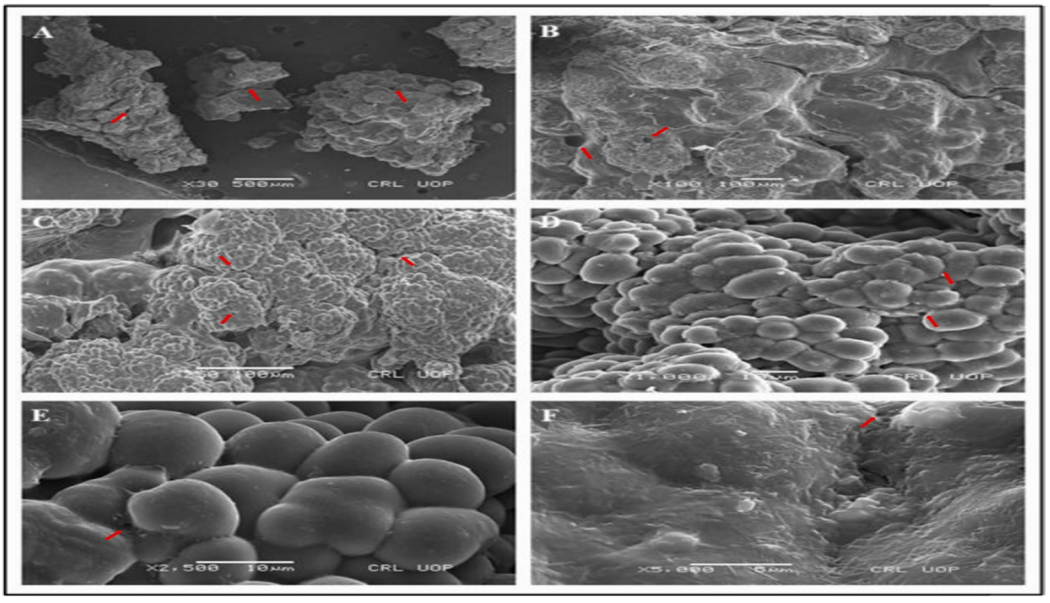

FIGURE 4.6: Scanning electron microscopy (SEM) images of the optimized hydrogel at increasing magnifications: (A) 30×, (B) 100×, (C) 250×, (D) 1000×, (E) 2500×, and (F) 5000×. Red arrows highlight porous networks.

4.7 Differential Scanning Calorimetry

Differential Scanning Calorimetry (DSC) analysis was performed to investigate the thermal behavior, crystallinity, and potential interactions between Capecitabine and the polymeric components of the optimally formulated hydrogel.

Cellulose acetate phthalate (CAP) showed a thermogram with a wide endothermic transition between 100°C and 150°C which might indicate moisture loss, or transition of glass to rubbery states (Tg). A slight peak at 400°C which was noted on the thermogram of CAP is the start for thermal degradation. Sharp endothermic peaks with 330°C and 350°C associated with its melting point confirm Capecitabine's crystalline structure as well as its thermal stability. Pectin showed exothermic peak ranges between 400-450°C, suggesting thermal degradation which is typical of natural polysaccharides, and an endothermic peak below 150°C, attributed to moisture evaporation. Guar gum displayed similar thermal profile of polysaccharide degradation and exothermic peaks around 450°C after initial endothermic transition below 150°C [112].

The thermogram of the unloaded hydrogel formulation exhibited broad, shifted peaks indicating the interactions between polymeric components that help form a stable matrix. The lack of melting point of capecitabine on this formulation suggests that the drug was indeed not used. Its broad transitions indicative of an amorphous structure support the formulation's ability for potential controlled drug release. On the other hand, the drug loaded hydrogel formulation seemed to lose or significantly diminish the melting peak of Capecitabine around 350°C. This suggests that the drug was successfully incorporated, transformed from a crystalline to an amorphous form. The endothermic transitions of the drug loaded formulation between 300°C and 400°C are likely due to some form of interaction, perhaps hydrogen bonds, between the drug and the polymer matrix. These thermal changes together with the loss of melting point of capecitabine suggest that drug is molecularly dispersed within the polymer matrix. This phenomenon enhances the formulation's stability, indicating a homogeneous system that ensures controlled drug release. The combination of pectin, guar gum, and CAP creates a

matrix that is stable and functional capable of sustaining drug release over an extended time. The formulations are suitable for standard manufacturing processes because they maintain thermal stability up to 300°C [113].

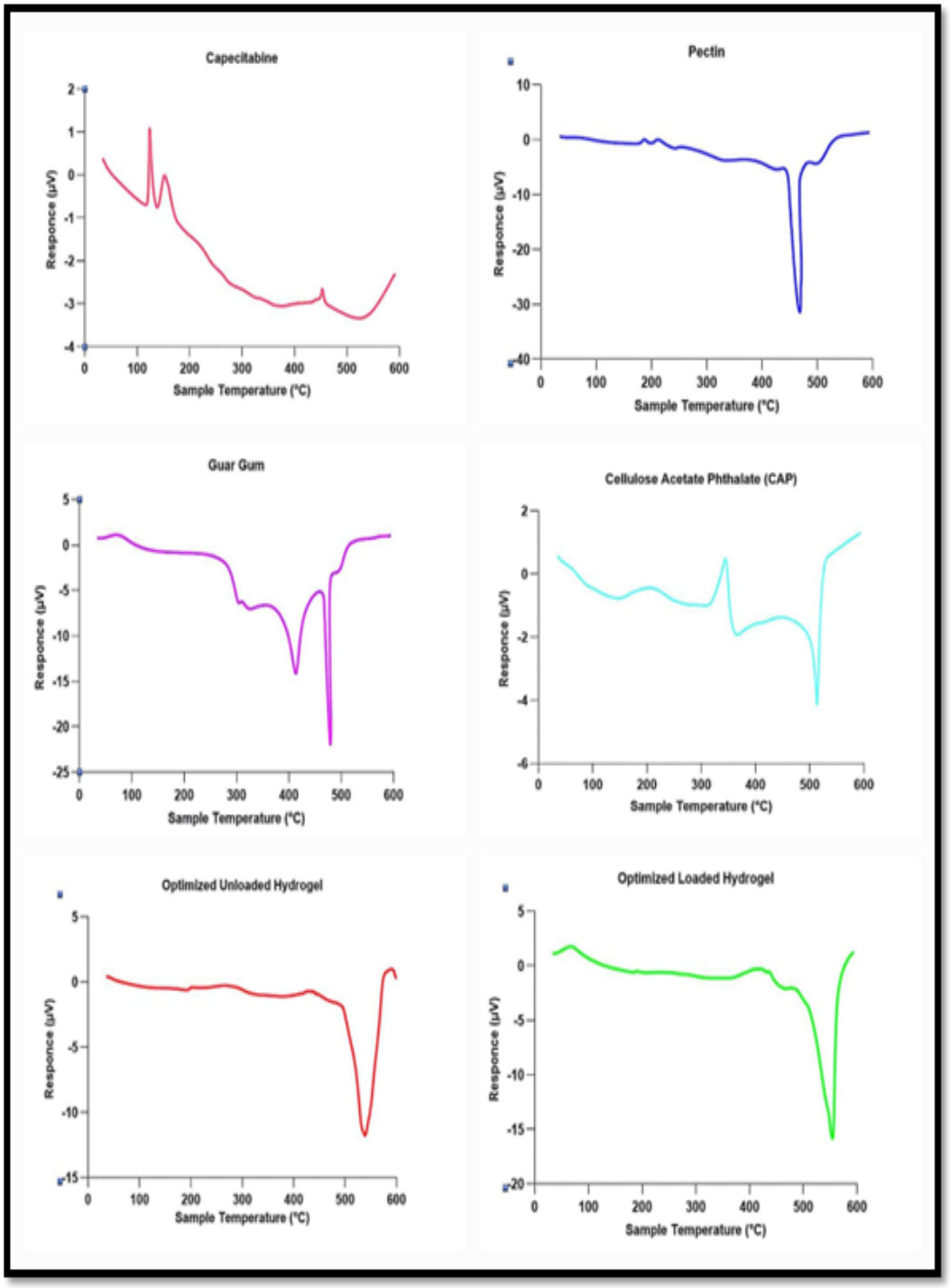

FIGURE 4.7: DSC thermograms of Capecitabine, Pectin, Guar Gum, Cellulose Acetate Phthalate (CAP), and the optimized unloaded and loaded hydrogel formulation. Y-axis scales vary to enhance the visibility of thermal events for each sample.

4.8 Acute Oral Toxicity Study

The acute oral toxicity study was conducted to evaluate the safety profile of the optimized hydrogel formulation. No mortality or overt signs of toxicity were observed in the treated group throughout the 14-day observation period, confirming the biocompatibility of the hydrogel as shown in. Fig 4.7. Regular body weight measurements at defined intervals showed no statistically significant differences ($p > 0.05$) between the treated and control groups, suggesting the absence of treatment-related metabolic disturbances [114].

Clinical parameters, including locomotor activity, grooming behavior, and food and water intake, remained within normal physiological ranges, further supporting the lack of adverse effects on neurological or metabolic functions depicted in Table 4.3.

Hematological analysis indicated that hemoglobin levels, total leukocyte counts, differential leukocyte counts, and platelet counts were within the normal physiological range, demonstrating that hydrogel administration did not induce hematopoietic abnormalities, as shown in Table 4.4. Statistical analysis of hematological and biochemical parameters revealed no significant differences between control and treated groups ($p > 0.05$, Student's t-test). Similarly, biochemical markers of liver function, including alanine aminotransferase (ALT), aspartate aminotransferase (AST), and alkaline phosphatase (ALP), remained comparable between the treated and control groups, ruling out any hepatotoxic effects. Renal function tests, including creatinine and urea levels, were also within reference limits, indicating no impairment in renal function. Histopathological examination of major organs (liver, kidneys, heart, spleen, stomach, and intestines) revealed preserved tissue architecture without structural abnormalities (Figure 4.8), cellular degeneration, or inflammatory infiltrates, further confirming the hydrogel's non-toxic nature The absence of systemic toxicity, hematological or biochemical alterations, and histopathological abnormalities supports the hydrogel's safety for oral administration and its suitability for further preclinical investigations [44].

Table 4.3: Clinical Observations in Acute Oral Toxicity Study

Parameter	**Group A (Control)**	**Group B (Treated)**	***Scale**
Body Weight (g)	Day 1: 25.5 ± 1.2 Day 7: 26.5 ±1.0 Day 14: 27.8 ± 1.3	Day 1: 25.2 ± 1.1 Day 7: 26.0 ± 1.2 Day 14: 27.5 ± 1.2	0: Normal increase (expected growth)
Food Intake (g/day)	Day 1: 4.5 ± 0.2 Day 7: 5.5 ± 0.3 Day 14: 6.0 ± 0.4	Day 1: 4.6 ± 0.3 Day 7: 5.4 ± 0.2 Day 14: 5.9 ± 0.3	0: Normal intake (no reduction)
Water Intake (mL/-day)	Day 1: 5.2 ± 0.4 Day 7: 6.0 ± 0.5 Day 14: 6.5 ± 0.6	Day 1: 5.3 ± 0.3 Day 7: 5.9 ± 0.4 Day 14: 6.4 ± 0.5	0: Normal intake (no reduction)
Locomotor Activity	Day 1: Normal Day 7: Normal Day 14: Normal	Day 1: Normal Day 7: Normal Day 14: Normal	0: Normal activity (no changes)
Grooming Behavior	Day 1: Normal Day 7: Normal Day 14: Normal	Day 1: Normal Day 7: Normal Day 14: Normal	0: Normal grooming behavior
Salivation	Day 1: Absent Day 7: Absent Day 14: Absent	Day 1: Absent Day 7: Absent Day 14: Absent	0: Absent (no salivation)
Piloerection	Day 1: Absent Day 7: Absent Day 14: Absent	Day 1: Absent Day 7: Absent Day 14: Absent	0: Absent (no piloerection)
Convulsions	Day 1: Absent Day 7: Absent Day 14: Absent	Day 1: Absent Day 7: Absent Day 14: Absent	0: Absent (no convulsions)
Lethargy	Day 1: Absent Day 7: Absent Day 14: Absent	Day 1: Absent Day 7: Absent Day 14: Absent	0: Absent (no lethargy)

Scale Definition: 0 = Normal;

1 = Mild Change (no significant impact on health or behavior);

2 = Moderate Change (observable effect, but still tolerable);

3 = Severe Change (significant impact on health or behavior)

TABLE 4.4: Biochemical Blood Analysis in Acute Oral Toxicity Study

Parameter	**Group A (Control) *(Mean ± SD)**	**Group B (Treated) *(Mean ± SD)**	**Normal Range**
Hemoglobin (g/dL)	13.5 ± 0.4	13.7 ± 0.3	12.0–15.0
WBC (10^3/mm^3)			
	7.2 ± 0.5	7.4 ± 0.4	5.0–10.0
White Blood Cells			
Platelets (10^3/mm^3)	250 ± 12	255 ± 10	150–400
ALT (U/L)			
	32.4 ± 2.3	31.8 ± 2.1	10–40
Alkaline Phosphatase			
AST (U/L)			
	28.5 ± 1.8	29.0 ± 1.7	10–50
AST			
ALP (U/L)			
	72.0 ± 3.4	73.2 ± 3.1	40–120
ALP			
Creatinine (mg/dL)	0.8 ± 0.05	0.81 ± 0.04	0.6–1.2
Urea (mg/dL)	22.1 ± 1.2	21.8 ± 1.3	15–40
Glucose (mg/dL)	92.3 ± 3.5	91.5 ± 3.2	70–110

Results are expressed as mean ± standard deviation (SD); n = 5 animals per group. All comparisons between treated and control groups showed no statistically significant differences ($p > 0.05$ by Student's t-test). Abbreviations: WBC - white blood cells; ALT - alanine aminotransferase; AST - aspartate aminotransferase; ALP - alkaline phosphatase.

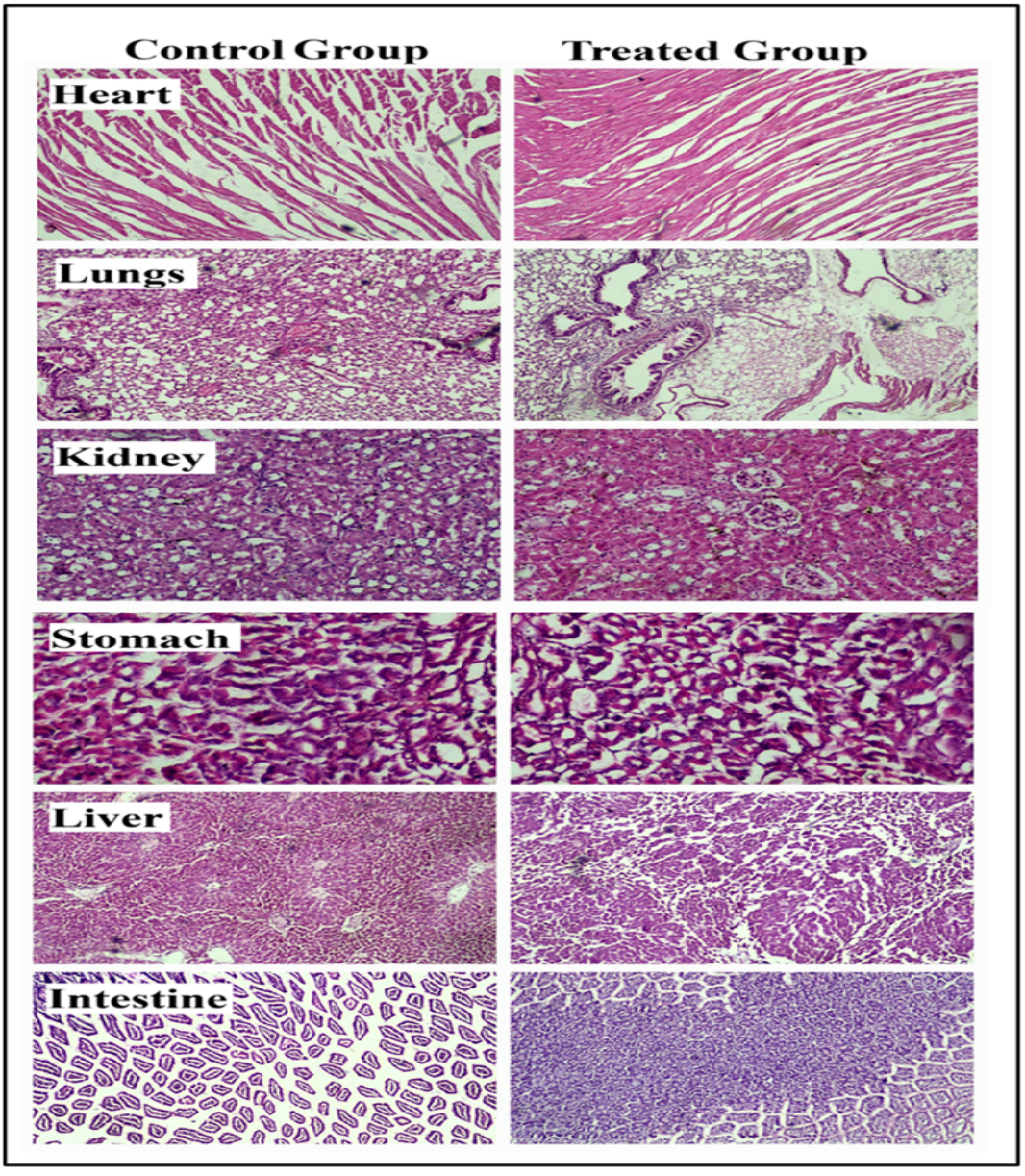

FIGURE 4.8: Histopathological evaluation of vital organs from control and treated groups. All organs exhibited preserved tissue architecture with no signs of cellular damage, inflammation, or structural abnormalities (H&E staining, 40× magnification).

Chapter 5

Conclusion and Future Recommendations

In this study, acrylic acid, cellulose acetate phthalate, guar gum, and pectin were successfully used to create a pH-responsive hydrogel system for the oral drug delivery of capecitabine. XRD analysis confirmed the drug's amorphous dispersion inside the hydrogel matrix, while FTIR spectroscopy demonstrated the chemical compatibility among the polymeric components. A highly porous structure was identified by SEM, which is crucial for attaining controlled drug release and improved swelling properties. The pH-dependent swelling behavior of the developed formulations ensured site-specific and controlled drug release under physiological settings. The formulation's biocompatibility was also validated by in vivo acute oral toxicity study, which showed no significant alterations on histopathological, biochemical, or hematological parameters. These findings collectively underscore the potential of the developed pH-responsive hydrogel system as a promising and clinically viable platform for the oral delivery of capecitabine, with the advantages of improved therapeutic efficacy and enhanced patient compliance. Based on these encouraging results, several directions are suggested for future work to build up on this research. To begin with, in vivo efficacy studies in suitable models of colorectal cancer should be performed to validate the therapeutic efficacy of the hydrogel under physiological conditions, such as targeting, bioavailability, and

anticancer effects. Secondly, consideration should be given to the mucoadhesive properties of the hydrogel system because increased adhesion to colonic mucosa could further enhance localized drug retention and therapeutic efficacy. The scalability of manufacturing should also be investigated through process optimization and stability evaluation under a range of environmental conditions with the goal of ensuring product reproducibility, scalability, and shelf life. Additionally, the versatility of the formulated hydrogel system may be explored by co-delivering several drugs, such as other anticancer agents or biologics, to test its applicability in combination therapy against multidrug-resistant or advanced-stage colorectal cancer. Formulating the hydrogel into patient-convenient oral dosage forms like capsules or coated tablets will improve acceptability as well as ease of delivery, especially in elderly or chronically sick patients. Finally, investigation into the interaction of the hydrogel with gut microbiota would give valuable information on its biodegradability, its possible impact on the microbial balance, and long-term safety, all of which are essential for use in a clinical setting. With ongoing research and development, this pH-sensitive hydrogel system has great potential for enhancing targeted drug delivery in the treatment of colorectal cancer and can potentially be a platform technology for delivering numerous therapeutic agents to the colon.

Bibliography

[1] R. Shukla and A. Tiwari, "Carbohydrate polymers: Applications and recent advances in delivering drugs to the colon," *Carbohydrate Polymers*, vol. 88, pp. 399–416, 2012.

[2] N. Anwar, F. Badar, and M. Yusuf, "Profile of patients with colorectal cancer at a tertiary care cancer hospital in pakistan," *Annals of the New York Academy of Sciences*, vol. 1138, pp. 199–203, 2008.

[3] M. Park, W. Li, A. Qureshi, and E. Cho, "Fat intake and risk of skin cancer in u.s. adults," *Cancer Epidemiology, Biomarkers & Prevention*, vol. 27, pp. 776–782, 2018.

[4] Q. Dai, C. Walkey, and W. Chan, "Polyethylene glycol backfilling mitigates the negative impact of the protein corona on nanoparticle cell targeting," *Angewandte Chemie International Edition*, vol. 53, pp. 5093–5096, 2014.

[5] Z. Housein, T. Kareem, and A. Salihi, "In vitro anticancer activity of hydrogen sulfide and nitric oxide alongside nickel nanoparticle and novel mutations in their genes in crc patients," *Scientific Reports*, vol. 11, pp. 1–11, 2021.

[6] R. Khallaf, H. Salem, and A. Abdelbary, "5-fluorouracil shell-enriched solid lipid nanoparticles (sln) for effective skin carcinoma treatment," *Drug Delivery*, vol. 23, pp. 3452–3460, 2016.

[7] P. Baindara, S. Korpole, and V. Grover, "Bacteriocins: Perspective for the development of novel anticancer drugs," *Applied Microbiology and Biotechnology*, vol. 102, pp. 10393–10408, 2018.

[8] H. Er, "Mechanisms of action of mesalazine in preventing colorectal carcinoma in inflammatory bowel disease," *[Journal Name Missing]*, vol. 18, pp. 10–14, 2003. Review article; journal name not specified.

[9] Y. Sun, Z. Zhao, Z. Yang, F. Xu, H. Lu, Z. Zhu, W. Shi, J. Jiang, P. Yao, and H. Zhu, "Risk factors and preventions of breast cancer," *International Journal of Biological Sciences*, vol. 13, pp. 1387–1397, 2017.

[10] Y. Park, S. Lee, S. Kim, Y. Liu, M. Lee, J. Shin, S. Seo, S. Kim, I. Kim, S. Lee, *et al.*, "Microrna-9 suppresses cell migration and invasion through downregulation of tm4sf1 in colorectal cancer," *International Journal of Oncology*, vol. 48, pp. 2135–2143, 2016.

[11] J. Prensner, W. Chen, M. Iyer, Q. Cao, T. Ma, S. Han, A. Sahu, R. Malik, K. Wilder-Romans, N. Navone, *et al.*, "Pcat-1, a long noncoding rna, regulates brca2 and controls homologous recombination in cancer," *Cancer Research*, vol. 74, pp. 1651–1660, 2014.

[12] J. Prensner, M. Iyer, O. Balbin, S. Dhanasekaran, Q. Cao, J. Brenner, B. Laxman, I. Asangani, C. Grasso, H. Kominsky, *et al.*, "Transcriptome sequencing across a prostate cancer cohort identifies pcat-1, an unannotated lincrna implicated in disease progression," *Nature Biotechnology*, vol. 29, pp. 742–749, 2011.

[13] F. Wang, X. Li, X. Xie, L. Zhao, and W. Chen, "Uca1, a non-protein-coding rna up-regulated in bladder carcinoma and embryo, influencing cell growth and promoting invasion," *FEBS Letters*, vol. 582, pp. 1919–1927, 2008.

[14] Y. Han, S. Ma, G. Yourek, Y. Park, and J. Garcia, "A transcribed pseudogene of mylk promotes cell proliferation," *FASEB Journal*, vol. 25, pp. 2305–2312, 2011.

[15] D. Herzig and V. Tsikitis, "Molecular markers for colon diagnosis, prognosis and targeted therapy," *Journal of Surgical Oncology*, vol. 111, pp. 96–102, 2015.

[16] P. Ohana, P. Schachter, B. Ayesh, A. Mizrahi, T. Birman, T. Scheneider, I. Matouk, S. Ayesh, P. Kuppen, N. de Groot, *et al.*, "Regulatory sequences of h19 and igf2 genes in dna-based therapy of colorectal rat liver metastases," *Journal of Gene Medicine*, vol. 7, pp. 366–374, 2005.

[17] K. Morris and J. Mattick, "The rise of regulatory rna," *Nature Reviews Genetics*, vol. 15, pp. 423–437, 2014.

[18] P. Schorderet and D. Duboule, "Structural and functional differences in the long non-coding rna hotair in mouse and human," *PLoS Genetics*, vol. 7, 2011.

[19] W. Li, J. Chang, S. Wang, X. Liu, J. Peng, D. Huang, M. Sun, Z. Chen, W. Zhang, W. Guo, *et al.*, "Mirna-99b-5p suppresses liver metastasis of colorectal cancer by down-regulating mtor," *Oncotarget*, vol. 6, pp. 24448–24462, 2015.

[20] I. Matouk, I. Abbasi, A. Hochberg, E. Galun, H. Dweik, and M. Akkawi, "Highly upregulated in liver cancer noncoding rna is overexpressed in hepatic colorectal metastasis," *European Journal of Gastroenterology & Hepatology*, vol. 21, pp. 688–692, 2009.

[21] L. Li, F. Jia, P. Bai, Y. Liang, R. Sun, F. Yuan, L. Zhang, and L. Gao, "Association between polymorphisms in long non-coding rna prncr1 in 8q24 and risk of gastric cancer," *Tumor Biology*, vol. 37, pp. 299–303, 2016.

[22] R. Yaeger, A. Cercek, E. O'Reilly, D. Reidy, N. Kemeny, T. Wolinsky, M. Capanu, M. Gollub, N. Rosen, M. Berger, *et al.*, "Pilot trial of combined braf and egfr inhibition in braf-mutant metastatic colorectal cancer patients," *Clinical Cancer Research*, vol. 21, pp. 1313–1320, 2015.

[23] A. d. Almeida, M. Bernardes, M. Feitosa, F. Peria, D. d. C. Tirapelli, J. d. Rocha, and O. Feres, "Serological under expression of microrna-21, microrna-34a and microrna-126 in colorectal cancer," *Acta Cirúrgica Brasileira*, vol. 31, pp. 13–18, 2016.

[24] Y. Song, Y. Xu, Z. Wang, Y. Chen, Z. Yue, P. Gao, C. Xing, and H. Xu, "Microrna-148b suppresses cell growth by targeting cholecystokinin-2 receptor in colorectal cancer," *International Journal of Cancer*, vol. 131, pp. 1042–1051, 2012.

[25] M. Rizwan, R. Yahya, A. Hassan, M. Yar, A. Azzahari, V. Selvanathan, F. Sonsudin, and C. Abouloula, "Ph sensitive hydrogels in drug delivery: Brief history, properties, swelling, and release mechanism, material selection and applications," *Polymers*, vol. 9, no. 4, 2017.

[26] P. Gupta, K. Vermani, and S. Garg, "Hydrogels: From controlled release to ph-responsive drug delivery," *Drug Discovery Today*, vol. 7, pp. 569–579, 2002.

[27] H. Brody, "Colorectal cancer," *Nature*, vol. 521, p. S1, 2015.

[28] A. Munro, S. Lain, and D. Lane, "P53 abnormalities and outcomes in colorectal cancer: A systematic review," *British Journal of Cancer*, vol. 92, pp. 434–444, 2005.

[29] S. Popat and R. Houlston, "A systematic review and meta-analysis of the relationship between chromosome 18q genotype, dcc status and colorectal cancer prognosis," *European Journal of Cancer*, vol. 41, pp. 2060–2070, 2005.

[30] X. Wang and Q. Zhang, "Ph-sensitive polymeric nanoparticles to improve oral bioavailability of peptide/protein drugs and poorly water-soluble drugs," *European Journal of Pharmaceutics and Biopharmaceutics*, vol. 82, pp. 219–229, 2012.

[31] M. Cristiano, F. Cilurzo, M. Carafa, and D. Paolino, *Innovative Vesicles for Dermal and Transdermal Drug Delivery*. Elsevier Inc., 2018.

[32] M. Qindeel, M. Ullah, F. ud Din, N. Ahmed, and A. u. Rehman, "Recent trends, challenges and future outlook of transdermal drug delivery systems for rheumatoid arthritis therapy," *Journal of Controlled Release*, vol. 327, pp. 595–615, 2020.

[33] P. Shanbhag and U. Jani, "Drug delivery through nails: Present and future," *New Horizons in Translational Medicine*, vol. 3, pp. 252–263, 2017.

[34] G. Sharma, K. Thakur, K. Raza, B. Singh, and O. Katare, "Nanostructured lipid carriers: A new paradigm in topical delivery for dermal and transdermal applications," *Critical Reviews in Therapeutic Drug Carrier Systems*, vol. 34, pp. 355–386, 2017.

[35] Y. Luo, Z. Teng, Y. Li, and Q. Wang, "Solid lipid nanoparticles for oral drug delivery: Chitosan coating improves stability, controlled delivery, mucoadhesion and cellular uptake," *Carbohydrate Polymers*, vol. 122, pp. 221–229, 2015.

[36] A. Vyas, S. Saraf, and S. Saraf, "Encapsulation of cyclodextrin complexed simvastatin in chitosan nanocarriers: A novel technique for oral delivery," *Journal of Inclusion Phenomena and Macrocyclic Chemistry*, pp. 251–259, 2010.

[37] A. Surana and R. Kotecha, "An overview on various approaches to oral controlled drug delivery system via gastroretention," *International Journal of Pharmaceutical Sciences Review and Research*, vol. 2, pp. 68–72, 2010.

[38] S. Kadowaki, M. Kakuta, S. Takahashi, A. Takahashi, Y. Arai, Y. Nishimura, T. Yatsuoka, A. Ooki, K. Yamaguchi, K. Matsuo, *et al.*, "Prognostic value of kras and braf mutations in curatively resected colorectal cancer," *World Journal of Gastroenterology*, vol. 21, no. 4, pp. 1275–1283, 2015.

[39] W. Li, T. Qiu, W. Zhi, S. Shi, S. Zou, Y. Ling, L. Shan, J. Ying, and N. Lu, "Colorectal carcinomas with kras codon 12 mutation are associated with more advanced tumor stages," *BMC Cancer*, vol. 15, pp. 1–7, 2015.

[40] V. Lao and W. Grady, "Epigenetics and colorectal cancer," *Nature Reviews Gastroenterology & Hepatology*, vol. 8, pp. 686–700, 2011.

[41] M. Pino and D. Chung, "The chromosomal instability pathway in colon cancer," *Gastroenterology*, vol. 138, pp. 2059–2072, 2010.

[42] N. Bastide, F. Pierre, and D. Corpet, "Heme iron from meat and risk of colorectal cancer: A meta-analysis and a review of the mechanisms involved," *Cancer Prevention Research*, vol. 4, pp. 177–184, 2011.

[43] J. Martinez-Useros and J. Garcia-Foncillas, "Obesity and colorectal cancer: Molecular features of adipose tissue," *Journal of Translational Medicine*, vol. 14, pp. 1–10, 2016.

[44] S. Shah, M. Sohail, M. Minhas, S. Khan, Z. Hussain, A. Mahmood, M. Kousar, and A. Mahmood, "Ti ti," 2019. Incomplete citation—please provide journal/book title.

[45] D. Chenthamara, S. Subramaniam, S. Ramakrishnan, S. Krishnaswamy, M. Essa, F. Lin, and M. Qoronfleh, "Therapeutic efficacy of nanoparticles and routes of administration," *Biomaterials Research*, vol. 23, pp. 1–29, 2019.

[46] N. Thombare, U. Jha, S. Mishra, and M. Siddiqui, "Guar gum as a promising starting material for diverse applications: A review," *International Journal of Biological Macromolecules*, vol. 88, pp. 361–372, 2016.

[47] Y. Che, D. Li, Y. Liu, Z. Yue, J. Zhao, Q. Ma, Q. Zhang, Y. Tan, Q. Yue, and F. Meng, "Design and fabrication of a triple-responsive chitosan-based hydrogel with excellent mechanical properties for controlled drug delivery," *Journal of Polymer Research*, vol. 25, 2018.

[48] L. Liu, Q. Gao, X. Lu, and H. Zhou, "In situ forming hydrogels based on chitosan for drug delivery and tissue regeneration," *Asian Journal of Pharmaceutical Sciences*, vol. 11, pp. 673–683, 2016.

[49] R. Jalababu, S. Satya Veni, and K. Reddy, "Development, characterization, swelling, and network parameters of amino acid grafted guar gum based ph responsive polymeric hydrogels," *International Journal of Polymer Analysis and Characterization*, vol. 24, pp. 304–312, 2019.

[50] X. Li, H. Wang, D. Li, S. Long, G. Zhang, and Z. Wu, "Dual ionically cross-linked double-network hydrogels with high strength, toughness, swelling resistance, and improved 3d printing processability," *ACS Applied Materials & Interfaces*, vol. 10, pp. 31198–31207, 2018.

[51] G. Lu, Y. Sun, S. An, S. Xin, X. Ren, D. Zhang, P. Wu, W. Liao, Y. Ding, and L. Liang, "Microrna-34a targets fmnl2 and e2f5 and suppresses the progression of colorectal cancer," *Experimental and Molecular Pathology*, vol. 99, pp. 173–179, 2015.

[52] Y. Qiu, H. Yu, X. Shi, K. Xu, Q. Tang, B. Liang, S. Hu, Y. Bao, J. Xu, J. Cai, *et al.*, "Microrna-497 inhibits invasion and metastasis of colorectal cancer cells by targeting vascular endothelial growth factor-a," *Cell Proliferation*, vol. 49, pp. 69–78, 2016.

[53] L. Sarli, L. Bottarelli, G. Bader, D. Iusco, S. Pizzi, R. Costi, T. D'Adda, M. Bertolani, L. Roncoroni, and C. Bordi, "Association between recurrence of sporadic colorectal cancer, high level of microsatellite instability, and loss of heterozygosity at chromosome 18q," *Diseases of the Colon & Rectum*, vol. 47, pp. 1467–1482, 2004.

[54] U. Rehman, R. Sarfraz, A. Mahmood, S. Akbar, A. Altyar, R. Khinkar, and H. Gad, "Ph responsive hydrogels for the delivery of capecitabine: Development, optimization and pharmacokinetic studies," *Gels*, vol. 8, 2022.

[55] N. Taleblou, M. Sirousazar, Z. Hassan, and S. Khaligh, "Capecitabine-loaded anti-cancer nanocomposite hydrogel drug delivery systems: In vitro and in vivo efficacy against the 4t1 murine breast cancer cells," *Journal of Biomaterials Science, Polymer Edition*, vol. 31, pp. 72–92, 2020.

[56] S. Agnihotri and T. Aminabhavi, "Novel interpenetrating network chitosan-poly(ethylene oxide-g-acrylamide) hydrogel microspheres for the controlled release of capecitabine," *International Journal of Pharmaceutics*, vol. 324, pp. 103–115, 2006.

[57] U. Rehman, R. Sarfraz, A. Mahmood, Z. Hussain, H. Thu, N. Zafar, M. Ashraf, and N. Batool, "Smart ph-responsive co-polymeric hydrogels for controlled delivery of capecitabine: Fabrication, optimization and in vivo toxicology screening," *Current Drug Delivery*, vol. 18, pp. 1256–1271, 2021.

[58] M. Upadhyay, H. Vardhan, and B. Mishra, "Natural polymers composed mucoadhesive interpenetrating buoyant hydrogel beads of capecitabine: Development, characterization and in vivo scintigraphy," *Journal of Drug Delivery Science and Technology*, vol. 55, p. 101480, 2020.

[59] U. Rehman, R. Sarfraz, A. Mahmood, T. Mahmood, N. Batool, B. Haroon, and Y. Benguerba, "Tamarind/-cd-g-poly(maa) ph responsive hydrogels for controlled delivery of capecitabine: Fabrication, characterization, toxicological and pharmacokinetic evaluation," *Journal of Polymer Research*, vol. 30, pp. 1–20, 2023.

[60] T. Yasmin, A. Mahmood, M. Farooq, U. Rehman, R. Sarfraz, H. Ijaz, M. Akram, A. Boublia, M. Salem Bekhit, B. Ernst, *et al.*, "Quince seed mucilage/-cyclodextrin/mmt-na$^+$-co-poly(methacrylate) based ph-sensitive polymeric carriers for controlled delivery of capecitabine," *International Journal of Biological Macromolecules*, vol. 253, p. 127032, 2023.

[61] I. Ahmed, A. Mahmood, O. Qureshi, R. Sarfraz, H. Ijaz, M. Zaman, M. Akram, S. Usmani, Zulcaif, and M. Malook, *Development of Tamarind Gum/-CD-co-poly(MAA) hydrogels for pH-driven controlled delivery of capecitabine*, vol. 81. Springer Berlin Heidelberg, 2024.

[62] T. Yasmin, A. Mahmood, R. Sarfraz, U. Rehman, A. Boublia, A. Alkahtani, G. Albakri, H. Ijaz, S. Ahmed, B. Harron, *et al.*, "Mimosa/quince seed mucilage–co-poly(methacrylate) hydrogels for controlled delivery of capecitabine: Simulation studies, characterization and toxicological evaluation," *International Journal of Biological Macromolecules*, vol. 275, p. 133468, 2024.

[63] U. Rehman, R. M. Sarfraz, A. Mahmood, S. Akbar, A. E. Altyar, R. M. Khinkar, and H. A. Gad, "PH Responsive Hydrogels for the Delivery of Capecitabine: Development, Optimization and Pharmacokinetic Studies," *Gels*, vol. 8, no. 12, p. 775, 2022.

[64] J. Seong, M. Yun, and S. Park, "Surfactant-stable and ph-sensitive liposomes coated with n-succinyl-chitosan and chitooligosaccharide for delivery of quercetin," *Carbohydrate Polymers*, vol. 181, pp. 659–667, 2018.

[65] M. Asad, D. Khan, A. Rehman, and A. Elaissari, "Development and in vitro / in vivo evaluation of ph-sensitive polymeric nanoparticles loaded hydrogel for the management of psoriasis," 2021. Journal name and volume not provided.

[66] M. Qindeel, N. Ahmed, F. Sabir, S. Khan, and A. Ur-Rehman, "Development of novel ph-sensitive nanoparticles loaded hydrogel for transdermal drug delivery," *Drug Development and Industrial Pharmacy*, vol. 45, pp. 629–641, 2019.

[67] M. Qindeel, N. Ahmed, F. Sabir, S. Khan, and A. Ur-Rehman, "Development of novel ph-sensitive nanoparticles loaded hydrogel for transdermal drug delivery," *Drug Development and Industrial Pharmacy*, vol. 45, no. 4, pp. 629–641, 2019.

[68] D. Peeler, D. Sellers, and S. Pun, "ph-sensitive polymers as dynamic mediators of barriers to nucleic acid delivery," *Bioconjugate Chemistry*, vol. 30, pp. 350–365, 2019.

[69] J. Seong, M. Yun, and S. Park, "Surfactant-stable and ph-sensitive liposomes coated with n-succinyl-chitosan and chitooligosaccharide for delivery of quercetin," *Carbohydrate Polymers*, vol. 181, pp. 659–667, 2018.

[70] I. Ahmad, M. F. A. Khan, A. Rahdar, S. Hussain, F. K. Tareen, M. W. Salim, N. Ajalli, M. I. Amirzada, and A. Khan, "Design and evaluation of ph sensitive peg-protamine nanocomplex of doxorubicin for treatment of breast cancer," *Polymers*, vol. 14, no. 12, p. 2403, 2022.

[71] K. Bashir, M. Farhan, A. Khan, A. Alhodaib, N. Ahmed, I. Naz, B. Mirza, M. Tipu, and H. Fatima, "Design and evaluation of ph-sensitive nanoformulation of bergenin isolated from bergenia ciliata," *Polymers*, 2022. Article details incomplete—volume and pages needed.

[72] C. Wang, Y. Ye, G. Hochu, H. Sadeghifar, and Z. Gu, "Enhanced cancer immunotherapy by microneedle patch-assisted delivery of anti-pd1 antibody," *Nano Letters*, vol. 16, pp. 2334–2340, 2016.

[73] C. Ramírez Barragán, E. Macías Balleza, L. García-Uriostegui, J. Andrade Ortega, G. Toríz, and E. Delgado, "Rheological characterization of new thermosensitive hydrogels formed by chitosan, glycerophosphate, and phosphorylated -cyclodextrin," *Carbohydrate Polymers*, vol. 201, pp. 471–481, 2018.

[74] Z. Wang, X. Han, Y. Wang, K. Men, L. Cui, J. Wu, G. Meng, Z. Liu, and X. Guo, "Facile preparation of low swelling, high strength, self-healing and ph-responsive hydrogels based on the triple-network structure," *Frontiers of Materials Science*, vol. 13, pp. 54–63, 2019.

[75] M. Ribeiro, A. Espiga, D. Silva, P. Baptista, J. Henriques, C. Ferreira, J. Silva, J. Borges, E. Pires, P. Chaves, *et al.*, "Development of a new chitosan hydrogel for wound dressing," *Wound Repair and Regeneration*, vol. 17, pp. 817–824, 2009.

[76] M. Hwang, J. Kim, J. Lee, Y. Kim, J. Kim, S. Chang, S. Jin, J. Kim, W. Lyoo, S. Han, *et al.*, "Gentamicin-loaded wound dressing with polyvinyl alcohol/dextran hydrogel: Gel characterization and in vivo healing evaluation," *AAPS PharmSciTech*, vol. 11, pp. 1092–1103, 2010.

[77] E. Lee, P. Balakrishnan, C. Song, J. Choi, G. Noh, and C. Park, "Microemulsion-based hydrogel formulation of itraconazole for topical delivery," *Korean Journal of Pharmaceutical Sciences*, vol. 40, no. 5, pp. 305–312, 2010.

[78] B. Kaith, R. Sharma, and S. Kalia, "Guar gum based biodegradable, antibacterial and electrically conductive hydrogels," *International Journal of Biological Macromolecules*, vol. 75, pp. 266–275, 2015.

[79] E. Ahmed, "Hydrogel: Preparation, characterization, and applications: A review," *Journal of Advanced Research*, vol. 6, pp. 105–121, 2015.

[80] B. Siddiqui, A. ur Rehman, R. Gul, I. Chaudhery, K. Shah, and N. Ahmed, "Folate decorated chitosan-chondroitin sulfate nanoparticles loaded hydrogel for targeting macrophages against rheumatoid arthritis," *Carbohydrate Polymers*, vol. 327, p. 121683, 2024.

[81] M. Lee, S. Seo, and J. Kim, "A -cyclodextrin, polyethyleneimine and silk fibroin hydrogel containing centella asiatica extract and hydrocortisone acetate: Releasing properties and in vivo efficacy for healing of pressure sores," *Clinical and Experimental Dermatology*, vol. 37, pp. 762–771, 2012.

[82] X. Li, Q. Yang, Y. Zhao, S. Long, and J. Zheng, "Dual physically crosslinked double network hydrogels with high toughness and self-healing properties," *Soft Matter*, vol. 13, pp. 911–920, 2017.

[83] H. Chen, X. Chang, D. Du, J. Li, H. Xu, and X. Yang, "Microemulsion-based hydrogel formulation of ibuprofen for topical delivery," *International Journal of Pharmaceutics*, vol. 315, pp. 52–58, 2006.

[84] P. Jiang, C. Yan, Y. Guo, X. Zhang, M. Cai, X. Jia, X. Wang, and F. Zhou, "Direct ink writing with high-strength and swelling-resistant biocompatible physically crosslinked hydrogels," *Biomaterials Science*, vol. 7, pp. 1805–1814, 2019.

[85] M. Champeau, V. Póvoa, L. Militão, F. Cabrini, G. Picheth, F. Meneau, C. Jara, E. de Araujo, and M. de Oliveira, "Supramolecular poly(acrylic acid)/f127 hydrogel with hydration-controlled nitric oxide release for enhancing wound healing," *Acta Biomaterialia*, vol. 74, pp. 312–325, 2018.

[86] P. Thoniyot, M. Tan, A. Karim, D. Young, and X. Loh, "Nanoparticle–hydrogel composites: Concept, design, and applications of these promising, multi-functional materials," *Advanced Science*, vol. 2, pp. 1–13, 2015.

[87] B. Nutan, A. Chandel, A. Biswas, A. Kumar, A. Yadav, P. Maiti, and S. Jewrajka, "Gold nanoparticle promoted formation and biological properties of injectable hydrogels," *Biomacromolecules*, vol. 21, pp. 3782–3794, 2020.

[88] M. Xia, Y. Cheng, Z. Meng, X. Jiang, Z. Chen, P. Theato, and M. Zhu, "A novel nanocomposite hydrogel with precisely tunable ucst and lcst," *Macromolecular Rapid Communications*, vol. 36, pp. 477–482, 2015.

[89] E. Giuliano, D. Paolino, M. Fresta, and D. Cosco, "Drug-loaded biocompatible nanocarriers embedded in poloxamer 407 hydrogels as therapeutic formulations," *Medicines*, vol. 6, no. 1, p. 7, 2018.

[90] Z. Chen, F. Liu, Y. Chen, J. Liu, X. Wang, A. Chen, G. Deng, H. Zhang, J. Liu, Z. Hong, *et al.*, "Targeted delivery of crispr/cas9-mediated cancer gene therapy via liposome-templated hydrogel nanoparticles," *Advanced Functional Materials*, vol. 27, pp. 1–9, 2017.

[91] I. Ullah, A. Farooq, I. Naz, W. Ahmad, H. Ullah, S. Sehar, and A. Nawaz, "Fabrication of polymeric hydrogels containing esomeprazole for oral delivery: In vitro and in vivo pharmacokinetic characterization," *Polymers*, vol. 15, no. 7, 2023.

[92] S. Malik, A. u. Rehman, M. Khan, N. Ahmed, and M. H. A. Nasir, "Solid lipid nanoparticles based topical hydrogel for potential treatment of infantile hemangioma," *Bionanoscience*, 2024.

[93] M. Patitsa, K. Karathanou, Z. Kanaki, L. Tzioga, N. Pippa, C. Demetzos, D. Verganelakis, Z. Cournia, and A. Klinakis, "Magnetic nanoparticles coated with polyarabic acid demonstrate enhanced drug delivery and imaging properties for cancer theranostic applications," *Scientific Reports*, vol. 7, pp. 1–8, 2017.

[94] T. Pivetta, S. Simões, M. Araújo, T. Carvalho, C. Arruda, and P. Marcato, "Development of nanoparticles from natural lipids for topical delivery of thymol: Investigation of its anti-inflammatory properties," *Colloids and Surfaces B: Biointerfaces*, vol. 164, pp. 281–290, 2018.

[95] A. Hasan, M. Socha, A. Lamprecht, F. E. Ghazouani, A. Sapin, M. Hoffman, P. Maincent, and N. Ubrich, "Effect of the microencapsulation of nanoparticles on the reduction of burst release," *International Journal of Pharmaceutics*, vol. 344, pp. 53–61, 2007.

[96] S. Hua, "Comparison of in vitro dialysis release methods of loperamide-encapsulated liposomal gel for topical drug delivery," *International Journal of Nanomedicine*, vol. 9, pp. 735–744, 2014.

[97] I. Rajput, F. Tareen, A. Khan, N. Ahmed, M. Khan, K. Shah, A. Rahdar, and A. Díez-Pascual, "Fabrication and in vitro evaluation of chitosan-gelatin based aceclofenac loaded scaffold," *International Journal of Biological Macromolecules*, vol. 224, pp. 223–232, 2023.

[98] B. Zhang and B. Yan, "Analytical strategies for characterizing the surface chemistry of nanoparticles," *Analytical and Bioanalytical Chemistry*, vol. 396, pp. 973–982, 2010.

[99] S. Kaufhold, A. Schippers, A. Marx, and R. Dohrmann, "Sem study of the early stages of fe-bentonite corrosion-the role of naturally present reactive silica," *Corrosion Science*, p. 108716, 2020.

[100] B. Shal, A. Khan, A. Khan, R. Ullah, G. Ali, S. Islam, I. Haq, H. Ali, E. Seo, and S. Khan, "Alleviation of memory deficit by bergenin via the regulation of reelin and nrf-2/nf-b pathway in transgenic mouse model," 2021.

[101] M. Farooq, F. Usman, M. Naseem, H. Aati, H. Ahmad, S. Manee, R. Khalil, K. u. R. Khan, M. Qureshi, and M. Umair, "Voriconazole cyclodextrin based polymeric nanobeads for enhanced solubility and activity: In vitro/in vivo and molecular simulation approach," *Pharmaceutics*, vol. 15, 2023.

[102] M. Ghadiri, S. Fatemi, A. Vatanara, D. Doroud, A. Najafabadi, M. Darabi, and A. Rahimi, "Loading hydrophilic drug in solid lipid media as nanoparticles: Statistical modeling of entrapment efficiency and particle size," *International Journal of Pharmaceutics*, vol. 424, pp. 128–137, 2012.

[103] M. Upadhyay, S. Adena, H. Vardhan, S. Yadav, and B. Mishra, "Development of biopolymers based interpenetrating polymeric network of capecitabine: A drug delivery vehicle to extend the release of the model drug," *International Journal of Biological Macromolecules*, vol. 115, pp. 907–919, 2018.

[104] S. Dash, P. Murthy, L. Nath, and P. Chowdhury, "Kinetic modeling on drug release from controlled drug delivery systems," *Acta Poloniae Pharmaceutica - Drug Research*, vol. 67, pp. 217–223, 2010.

[105] F. Munarin, M. Tanzi, and P. Petrini, "Advances in biomedical applications of pectin gels," *International Journal of Biological Macromolecules*, vol. 51, pp. 681–689, 2012.

[106] S. Kabir, P. Sikdar, B. Haque, M. Bhuiyan, A. Ali, and M. Islam, "Cellulose-based hydrogel materials: Chemistry, properties and their prospective applications," *Progress in Biomaterials*, vol. 7, pp. 153–174, 2018.

[107] F. Sahle, M. Giulbudagian, J. Bergueiro, J. Lademann, and M. Calderón, "Dendritic polyglycerol and n-isopropylacrylamide based thermoresponsive nanogels as smart carriers for controlled delivery of drugs through the hair follicle," *Nanoscale*, vol. 9, pp. 172–182, 2017.

[108] R. Negrulj, A. Mooranian, N. Chen-Tan, H. Al-Sallami, M. Mikov, S. Golocorbin-Kon, M. Fakhoury, G. Watts, F. Arfuso, and H. Al-Salami, "Swelling, mechanical strength, and release properties of probucol microcapsules with and without a bile acid, and their potential oral delivery in diabetes," *Artificial Cells, Nanomedicine, and Biotechnology*, vol. 44, pp. 1290–1297, 2016.

[109] I. Kim, J. Park, I. Cheong, and J. Kim, "Swelling and drug release behavior of tablets coated with aqueous hydroxypropyl methylcellulose phthalate (hpmcp) nanoparticles," *Journal of Controlled Release*, vol. 89, pp. 225–233, 2003.

[110] H. Lin, P. Wang, W. Zhang, H. Yan, H. Yu, L. Yan, H. Chen, M. Xie, and L. Shan, "Novel combined preparation and investigation of bergenin-loaded albumin nanoparticles for the treatment of acute lung injury: In vitro and in vivo evaluations," *Inflammation*, vol. 45, pp. 428–444, 2022.

[111] S. Raman, A. Khan, and S. Mahmood, "Nose to brain delivery of selegiline loaded plga/lipid nanoparticles: Synthesis, characterisation and brain pharmacokinetics evaluation," *Journal of Drug Delivery Science and Technology*, vol. 77, p. 103923, 2022.

[112] R. Pignatello, P. Simerska, A. Leonardi, A. Abdelrahim, G. Petronio, V. Fuochi, P. Furneri, B. Ruozi, and I. Toth, "Synthesis, characterization and in vitro evaluation of amphiphilic ion pairs of erythromycin and kanamycin antibiotics with liposaccharides," *European Journal of Medicinal Chemistry*, vol. 120, pp. 329–337, 2016.

[113] G. Shevalkar and P. Vavia, "Solidified nanostructured lipid carrier (s-nlc) for enhancing the oral bioavailability of ezetimibe," *Journal of Drug Delivery Science and Technology*, vol. 53, p. 101211, 2019.

[114] S. Das, N. Debnath, S. Mitra, A. Datta, and A. Goswami, "Comparative analysis of stability and toxicity profile of three differently capped gold nanoparticles for biomedical usage," *BioMetals*, vol. 25, pp. 1009–1022, 2012.